その他研究分担者の発表論文

研究課題名：自由電子レーザーの殺細胞効果に関する研究

研究代表者：田中 良明 (日本大学医学部)

(1) 田中良明,河守次郎,平山道子,前林俊也,; "放射線感受性を高めるための臨床的工夫", 癌の臨床, 2000, 46(3), 219-222

(2) Hiraoka M, Mitsumori M, Hiroi N, Ohno S, Tanaka Y, Kotsuka Y, Sugimachi K,; "Development of RF and microwave heating equipment and clinical applications to cancer treatment in Japan", IEEE Transactions on Microwave Theory and Techniques, 2000, 48(11),1789-1799

(3) 遠藤壮平,濱田敬永,鴨原俊太郎,渡辺佳治,中里秀史,渡辺健一,鈴木伸,野口雄五,木田亮紀,田中良明,河守次郎,;"進行下咽頭･頸部食道癌に対する照射化学療法の検討",頭頸部腫瘍,2001,27(1), 1-8

(4) Karasawa K, Kaizu T, Niibe Y, Ishikawa H, Okamura T, Tanaka Y,; "Intrathoracic thermochemoradiotherapy for the treatment of locally-advanced malignant pleural mesothelioma-Treatment protocol and report of the three cases", Jpn J Hyperthermic Oncol, 2001, 17(1), 45-52

(5) 藤井元彰,田中良明,河守次郎,島田裕司,中村道子,前林俊也,早坂和正,奥畑好孝,;"ライナックによるエックスナイフを用いた定位放射線照射の現状と展望",日大医学雑誌, 2001,60(3), 162

(6) Niibe Y, Karasawa K, Kaizu T, Ieki R, Ishikawa H, Tanaka Y,; "Three-dimensional conformal radiation therapy for lung tumors using a middle fraction size: Preliminary results", J Jpn Soc Ther Raiol Oncol, 2003, 15(1),17-21

(7) Karasawa K, Kaizu T, Niibe Y, Igaki H, Shinohara M, Tanaka Y, Matsuda T,; "Rotational 3D-conformal radiation therapy (conformation therapy) combined with hormone therapy for the treatment of stage B2/C prostate cancer in Japanese men", Int J Radiat Oncol Biol Phys, 2003, 56(1), 208-212

(8) 田中良明,; "原体照射発展の足跡と今後の展開", 日放腫会誌, 15(4), 251-262

(9) Niibe Y, Karasawa K, Nakamura O, Shinoura N, Okamoto K, Yamada R, Fukino K, Tanaka Y.; "Survival benefit of stereotactic radiosurgery for metastatic brain tumors in patients with controlled primary lesions and no other distant metastases", Anticancer Res, 2003, 23(5b), 4157-4159

(10) Yokoyama T, Yoshino A, Katayama Y, Watanabe T, Kashima Y, Yoshikawa T, Kawamori J, Tanaka Y,; "Metastatic pituitary tumor from renal cell carcinoma treated by fractionated stereotactic radiotherapy-case report-", Neurol Med Chir (Tokyo), 2004, 44(1), 47-52

研究課題名：電子線による遺伝子損傷に関する研究

研究代表者：茂呂 周 (日本大学歯学部)

(1) Y.NAKAMURA, S.NOSAKA, M.SUZUKI, NAGAFUCHI, T.TAKAHASHI, T.YAJIMA, N.TAKENOUCHI-OHKUBO, T.IWASE and I.MORO. Dietary fructooligosaccharides up-regulate immunoglobulin A response and polymeric immunoglobulin receptor expression in intestines of infant mice. Clin Exp Immunol 2004; 137: 52-58

(2) Arihiro Iwata, Takashi Iwase, Yoshitaka Ogura, Tomihisa Takahashi, Naoyuki Matsumoto, Toshiyuki Yoshida, Nobuhiro Kamei, Kunihiko Kobayashi, Jiri Mestecky, Itaru Moro. Cloning and expression of the turtle (Trachemys scripta) immunoglobulin joining (J)-chain cDNA. Immunogenetics (2002) 54:513-519

(3) T. Takahashi, M. Kimura, N. Matsumoto, A. Iwata, Y. Ogura, T. Yoshida, N. Kamei, K. Komiyama, J. Mestecky, and I. Moro. Cloning of the Chicken Immunoglobulin Joining (J)-Chain Gene and Characterization of its Promoter Region. DNA and Cell Biology, 21(2), 2002, 81-90

Development of RF and Microwave Heating Equipment and Clinical Applications to Cancer Treatment in Japan

Masahiro Hiraoka, Michihide Mitsumori, Naotoshi Hiroi, Shinji Ohno, Yoshiaki Tanaka, Youji Kotsuka, *Senior Member, IEEE*, and Keizo Sugimachi

***Abstract*—Development of RF and microwave (MW) heating equipment for hyperthermia and their clinical applications to various cancers undertaken in Japan have been reviewed in this paper. Originally developed heating devices include an RF capacitive and RF inductive heating device, an MW heating device with a lens applicator, an RF intraluminal heating device, an RF current interstitial heating device, and a ferromagnetic implant heating device. The concept and characteristics of those devices are described herein. Nonrandomized and randomized trials undertaken for superficial and deep-seated tumors demonstrated improved local response with the combined use of hyperthermia. Furthermore, the complications associated with treatment were not generally serious, except for chronic bowel damages suggested in a trial for colorectal cancers. These clinical results indicate the benefit of combined treatment of hyperthermia and radiotherapy. With the advancement of heating and thermometry technologies, hyperthermia will be more widely and safely used in the treatment of cancers.**

***Index Terms*—Capacitive heating, clinical trial, hyperthermia, inductive heating, intaluminal heating, interstitial heating.**

I. Introduction

DURING THE past two decades, hyperthermia in combination with radiotherapy or chemotherapy has been investigated basically and clinically as a new cancer treatment modality. Numerous biological experiments demonstrate strong biological rationale for the use of hyperthermia in cancer therapy [1], [2].

Problems related to the physics and engineering of hyperthermia have also been investigated. Many kinds of heating techniques and methods for accurately measuring temperature inside the human body have been studied, particularly in the past decade. Most of these efforts seem to have been focused on the development of an applicator capable of heating deep tumors with accuracy. However, there are several problems that make it difficult to achieve deep and accurate heating. These problems include skin-depth restriction based on the skin effect and the presence of insulating materials such as lipid, protein, and bones in the human body for dielectric-type heating. In addition, eddy currents cause hot spots in unexpected regions.

As for techniques of measuring temperature, both invasive and noninvasive methods have been investigated. Invasive thermometers need lead wires to couple them either electrically or optically to an external monitor. The invasive thermometers must be sterilized prior to insertion into the patient. The patient tolerance for needle insertion is often low, limiting the number of measurement points in the tumor and, thus, limiting the thermal dose assessment. Among invasive methods, there are thermometers using thermocouples, thermistor, and fluorescent materials. Noninvasive thermometers include those that explore the use of magnetic resonance imaging (MRI) and microwave (MW) radiometry [3], [4]. These promising methods are under development.

In Japan, development of heating devices have been intensively investigated, including an RF capacitive and an microwave heating (MWH) device with a lens applicator, an RF intraluminal heating device, an RF current interstitial heating device, a ferromagnetic implant heating device, and MW interstitial heating devices. The former three devices have been approved as medical equipment for the clinical use from the Ministry of Health and Welfare of Japan. Hyperthermic treatment for cancer using electromagnetic (EM) waves is now covered by health insurance in Japan, and a large amount of clinical data has been accumulated. In this paper, we will discuss heating devices developed in Japan, and also describe the current status of clinical applications in cancer therapy.

II. Heating Devices

Various techniques for producing localized or regional hyperthermia, including annular array using MWs, inductive RF heating, and capacitive RF heating have been developed. However, each technique has its own inherent advantage and disadvantage, and its use should be chosen based on its clinical site and tissue composition. Heating methods are divided into external, intraluminal, and interstitial heating.

A. External Heating Devices

1) Dielectric-Type Heating: External heating administers heat to the tumor through various body structures. Delivery of heat energy to superficially located tumors is relatively easy.

Manuscript received October 30, 1999; revised May 20, 2000.

M. Hiraoka, M. Mitsumori, and N. Hiroi are with the Department of Therapeutic Radiology and Oncology, Graduate School of Medicine, Kyoto University, Kyoto 606-8507, Japan.

S. Ohno and K. Sugimachi are with the Department of Surgery II, Kyushu University, Fukuoka 812-8582, Japan.

Y. Tanaka is with the Department of Radiology, Nihon University School of Medicine, Tokyo 173- 8610, Japan.

Y. Kotsuka is with the Department of Telecommunications, Faculty of Engineering, Tokai University, Kanagawa 259-1292, Japan (e-mail: ykotsuka@keyaki.cc.u-tokai,ac.jp).

Publisher Item Identifier S 0018-9480(00)09529-6.

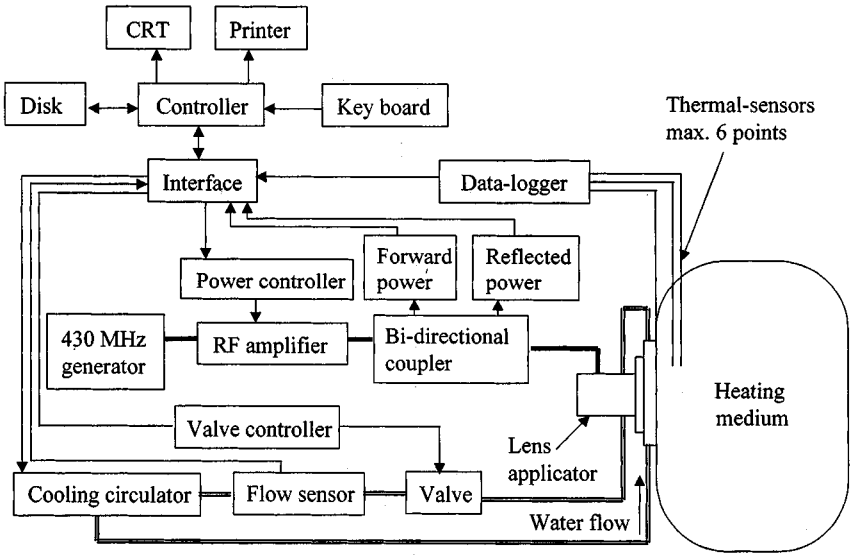

Fig. 1. 430-MHz MW heating equipment with a lens applicator.

MWH is most prevalently used for external heating of superficial tumors. One of the major problems of MWH is that the depth penetration is limited by the principle of skin-depth theory in EM wave. Only tumors located 2-3 cm from the skin surface can, therefore, be heated with a conventional surface applicator [5].

To attain deeper localized heating, metal-plate lens applicators have been developed in Japan that can converge MW energy in a lossy medium, such as human muscle, with a computer-controlled heating system [6]. Calculation of an electric-field distribution [7] and heating experiment in phantoms and miniature pigs [8] actually demonstrated a maximum heating depth of up to 6 cm with this device, which is approximately twice as deep as that obtained with a conventional waveguide applicator. This hyperthermia system consists of a 430-MHz MW generator unit with maximum output power of 500 W, a surface cooling unit, a thermometry unit, an applicator unit, and microcomputer-controlling system, as shown in Fig. 1. A four-aperture lens applicator with a total aperture size of 212 $\times$ 80 mm or a two-aperture lens applicator with a total size of 100 $\times$ 50 mm is available. The applicator is covered with a water bag, in which deionized water is circulating. The skin-surface temperature is controlled by changing the temperature of the circulating water from 10 °C–50 °C. The temperature is measured by a single-point or multipoint thin Teflon-coated copper-constant thermocouple sensor with an outer diameter of 0.8 mm. A multisensor has 3–6 separate thermocouples, with junctions located at 6-, 8-, or 10-mm intervals. During hyperthermia, MW power is switched off for 5 s every 24 s for temperature measurement.

Heat delivery to deep seated is more challenging, and major efforts have been devoted to the development of external deep-heating equipment. The ideal heating device should be capable of raising the whole tumor volume to a therapeutic temperature without overheating adjacent normal tissues.

Regional heating is the most commonly used deep-heating method. Since regional heating techniques apply energy to the adjacent deep-seated tumors in an unfocused manner, energy is also delivered to the adjacent normal tissues. Under such conditions, selective heating of tumors is only possible when heat dissipation by blood flow in normal tissue is greater than that in tumor tissue. An annular phased-array system delivering 60–80-MHz EM waves and RF capacitive heating apparatus are examples of regional heating devices. The former system has the advantage in that subcutaneous fat is not excessively heated and, thus, it is suitable for obese patients. However, this method causes systemic symptoms such as tachycardia and malaise, which result from the use of large-sized applicators. Systemic stress is reported to be more severe in patients with abdominal tumors than in those with pelvic tumors or tumors of the extremities [9], suggesting limited usefulness of this heating modality for tumors in the upper abdomen.

An 8-MHz RF capacitive heating device has been developed with a grant from the Research Development Corporation of Japan [10]. The device is schematically illustrated in Fig. 2. This equipment was approved as a medical device for thermotherapy of cancer by the Japanese Ministry of Health and Welfare in December 1984, and is now installed at over 100 hospitals in seven countries. Physical characteristics of this heating method has been described [11]. It has a self- excited oscillation circuit at 8 MHz and 1.5-kW maximum output power. The RF energy is transmitted from a generator via two coaxial cables to two disc electrodes. The RF is applied through a pair of electrodes placed on opposite sides of the body and the power is distributed locally or regionally through interaction of electric fields produced between the parallel-opposed electrodes. To facilitate heating of any site of the body, the gantry with the electrode can be rotated 180°. The adjustable positions of the electrodes and the rotation of the gantry permit heating at different angles and treatment sites. The treatment couch is motorized for vertical and horizontal movement. A portion of the top panel of the couch is opened electrically, and the lower electrode is protruded through the opening when vertical coupling is used. A pair of electrodes is connected to the pillars of the gantry. The surface of the metal plate of the electrodes is covered with a flexible water pad. Temperature-controlled water is flowing through

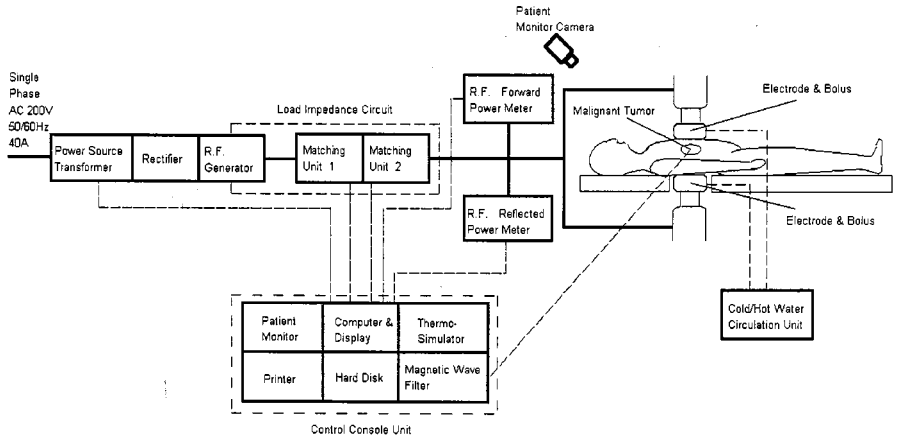

Fig. 2. 8-MHz RF capacitive heating device.

the water pad so that excessive heating of the skin and subcutaneous fat can be avoided. This pad makes it possible to smoothly attach the electrodes to the body surface. Thus, the RF energy can be supplied relatively homogeneously to an uneven site on the body. The water temperature is maintained at 30 °C–40 °C for superficial tumors and at approximately 10 °C for subsurface or deep tumors. The electrodes vary from 4–30 cm in diameter. Suitable electrodes are selected according to the size and location of the tumors. This capacitive applicator has a thermometry system with four Teflon-coated probes of copper-constant microthermocouple. The thermometry system with the microthermocouples connected to an automatic temperature-power feedback controller provides an accuracy of 0.2 °C. The high RF wave filter is inserted in the thermometry system, which is nonperturbed by RF interference and makes it possible to measure temperature even during heating. Studies made at the Minnesota University Hospital demonstrated that the measured temperature fluctuation was less than 0.45 °C when the RF current was turned on and off [12]. The temperatures measured at four points in the heated tissue are continuously displayed both graphically and digitally on the computer screen. These data are also continuously recorded on a hard disc drive, and a hard copy can be obtained on the internal printer. The power absorbed by the heated site is also continuously displayed graphically and digitally, and is recorded. An example of a thermal distribution in a human tumor treated with this device is shown in Fig. 3.

The disadvantage of RF capacitive heating is the excessive heating of subcutaneous fat, and it is shown that a patient with subcutaneous fat of more than 1.5–2 cm in thickness is difficult to heat with this heating modality [13]. The advantages are its wide applicability to various anatomical sites and relatively small systemic stress.

For tumor sites such as the neck region, where only a small amount of subcutaneous fat is present, localized RF heating will be advantageous. In dielectric-type RF applicators using a pair of circular conductive electrodes, a large-size electrode is usually needed to deeply heat a tumor uniformly. In the case of a capacitive applicator with a pair of circular electrodes, a diameter of more than 1.5 times the space between both electrodes is needed to achieve uniform heating inside the human body. For example, if the height of the heating region is 15 cm, 22.5 cm is needed as the diameter of the electrode to uniformly heat the human body in this area. If the diameter is less than this, hot spots will arise and the device cannot heat deeply.

(a)

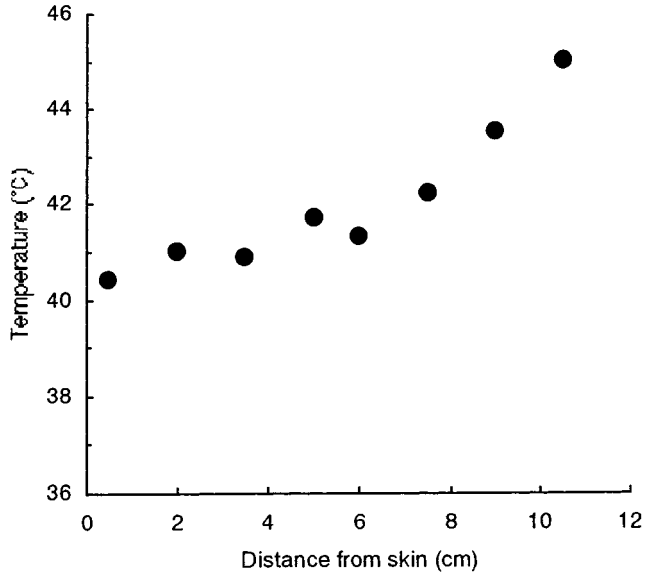

(b)

Fig. 3. Thermal distribution of an abdominal huge tumor (MHF) treated with an RF capacitive heating device. (a) Thin catheter for the guidance of a thermometer is demonstrated in the CT image. (b) Thermal distribution was obtained by pulling out the thermometer by a 5-cm step.

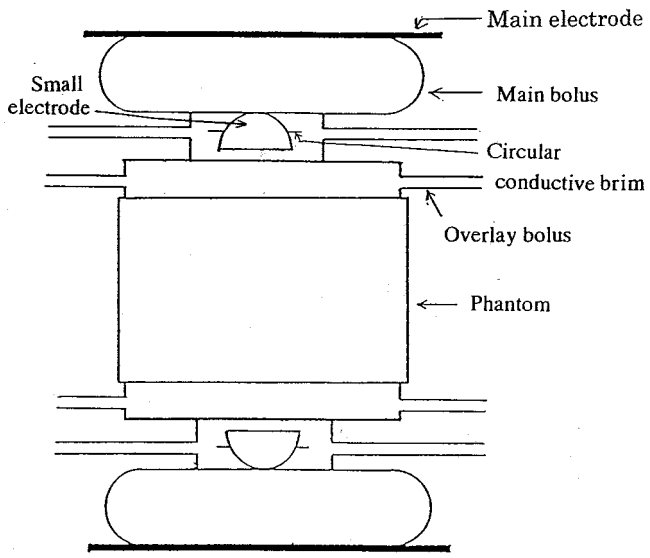

Fig. 4. Construction of new applicator with double electrodes.

To improve this, a capacitive applicator with a double electrode has been developed to achieve local heating, as shown in Fig. 4 [14]. By introducing a subelectrode consisting of a ferrodielectric material under the main electrode, an electric field can be concentrated between a pair of subelectrode or ferrodielectric materials. The size of the beam spot is proportional to the diameter of the semicircular subelectrode. If the semicircular subelectrode of 5 cm in diameter is used, a 5-cm beam of electric field over a distance of 20 cm between a pair of electrodes can be obtained.

2) Inductive Heating: Since magnetic fields in RF inductive heating can penetrate an insulating material such as subcutaneous fat, it can heat a tumor without heating fat tissue. A simple aperture-type applicator has been proposed using a one-turn square column-like coil made of a metal strip [15]. The operating frequency and maximum output power are 6 MHz and 7 kW, respectively. The experiment using living pigs and the clinical trials are investigated in [16] and [17].

Generally, it is difficult to achieve deep inductive heating because the eddy currents are predominantly induced near the surface of the human body. To resolve this problem, a deformed ferrite core applicator system with auxiliary electrode has been developed [18]. The operating frequency and the output power are 4 MHz and 850 W, respectively.

Deep local inductive heating can be achieved using an implant material, which generates heat by its interaction with the magnetic field. However, since eddy currents are predominantly induced near the surface of the human body, the result is that both the implanted region and superficial normal tissue are being heated. To reduce the heating of normal superficial tissue, an eddy-current absorber has been proposed [19]. This eddy-current absorber consists of silicon rubber containing a fine carbon powder. By optimizing material constant of the eddy-current absorber, the eddy currents that arise at unexpected portion of the human body can be absorbed.

Knowing that a ferrite core applicator is able to efficiently heat the inside of a protuberance on the human body, a simple applicator using a pair of ferrite cores has been developed for breast hyperthermia [19]. This applicator can regionally heat the breast, regardless of the size of the breast, without overheating fat tissue.

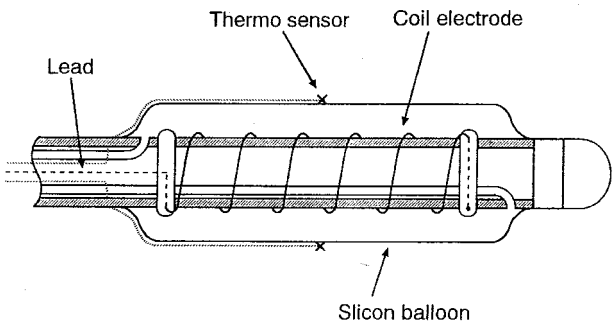

Fig. 5. Intralumonal RF electrode.

B. Intraluminal Heating Devices

The second method for deep heating is an intraluminal heating using hot fluid, MW, or RF. Sugimachi *et al.* [20] have developed an RF intraluminal hyperthermia system. Very localized heating is possible with this device by inserting an endotract electrode into lumens of the human body, such as the esophagus, rectum, and uterine cervix. A wide counter electrode is placed on the skin surface of the body so that the RF flux concentrates around the endotract electrode. Various types of electrodes are available depending on the size of the lumen and the site of the lesion. An electrode is connected to the RF system, which is operated at the frequency of 13.56 MHz with a maximum power of 250 W. The main structure of the electrode consists of the following three parts, as shown in Fig. 5:

1) transmitter for RF irradiation;
2) balloon and cooling system, which eliminates the gap between malignant tissues and the transmitter (60 ml/min of water at the room temperature is circulated to prevent overheating of the transmitter);
3) thermosensor: copper/constant microthermocouples were fixed to the outside of the balloon.

Recently, a new intraluminal electrode has been developed that enables us to undertake simultaneous thermoradiotherapy. A high-dose rate irradiation source (192 Ir) can be introduced inside this electrode.

C. Interstitial Heating Devices

The third method is interstitial heating, which is divided into RF current heating, MWH, and ferromagnetic implant heating. The advantages of interstitial heating are: 1) selective heating of localized tumors and 2) feasibility of combined use of brachytherapy. On the other hand, the disadvantages are: 1) invasiveness; 2) difficulty in repeated treatment; and 3) limitation of applicable sites.

As an interstitial heating devices, a fine coaxial line with small slots of about 1 mm in a outer conductor has been developed [21]–[23]. The operating frequency is 430 MHz. Ferromagnetic implant heating is being investigated in Japan. They have developed an implant heating system (IHS), which consists

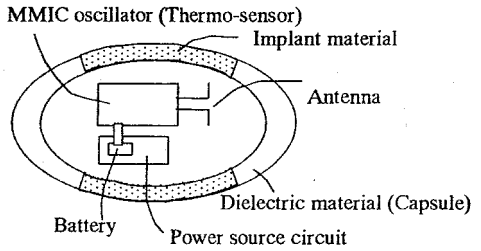

Fig. 6. Wireless thermometer with implant function using a three-dimensional MMIC.

of a ferromagnetic implant, induction coil, and generator to produce a high-frequency magnetic field. The implant is made of Fe–Pt alloy (Fe: 73%, Pt: 27%), and has a Curie temperature of 68 °C. This system is being clinically investigated for the treatment of brain tumors [24] and tongue cancers [25].

One of the important problems to overcome in hyperthermia is to achieve an accurate deep local heating together with exact measurements of temperature. A wireless-thermometer using a monolithic microwave integrated circuit (MMIC) with an implant function has been proposed from these viewpoints [26], as shown in Fig. 6. As a temperature sensor, a silicone MMIC with a voltage-controlled oscillator (Si MMIC VCO) has been introduced. Its size is very small, i.e., 2×2 mm. This has a special feature in that the thermometer is a very simple construction because the Si MMIC VCO acts as a temperature sensor, thus, the thermometer can be constructed without a transmitter or amplifier. As a wireless thermometer, it can measure the temperature accurately without noise interference induced by a lead wire carrying irradiated EM waves from an applicator.

III. Clinical Applications: Superficial and Subsurface Tumors

A large number of clinical experiences with combined hyperthermia and radiation therapy have been reported for superficial and subsurface tumors. Treatment of superficial tumors offer significant advantage as compared to the treatment of deep-seated tumors. Well-developed heating devices are available for their treatment, and these tumors are easy to both heat and to place thermometers into. The response of superficial tumors to the combined treatment is relatively easy to assess and, therefore, they provide a good model to investigate the combined effectiveness of hyperthermia and radiation. Additionally, several superficial tumors, including malignant melanoma, soft-tissue tumors, locally advanced tumors, and recurrent tumors following radiation therapy are still resistant to conventional treatments. The combined hyperthermia and radiation therapy offers potential clinical advantages for the treatment of these tumors.

Usefulness of thermoradiotherapy was initially demonstrated by several trials, including our trial in patients with two or more comparable tumors (matched tumors) [27]. Approximately a twofold increase in local response rates was shown in thermoradiotherapy than in radiotherapy alone. In addition to these studies, prospective randomized trials have been recently performed. A trial carried out by the Radiation Therapy Oncology Group (RTOG) in the U.S. failed to show a difference in the response rate between radiation alone and radiation plus heat when the tumors treated were analyzed all together [28]. When the tumor response was assessed according to the tumor size, a significantly higher response rate was achieved with the combined hyperthermia and radiotherapy for tumors with maximum diameter less than 3 cm, but not for tumors more than 3 cm in diameter. On the other hand, however, it was pointed out that to evaluate tumor response after the thermoradiotherapy, appearance of low-density area (LDA) on computed tomography (CT) images are more important than the actual shrinkage of tumor volume [29]. The combined treatment also showed a substantially higher response rate in breast tumors, but not in head and neck tumors or other tumors in comparison with radiotherapy alone. Since smaller tumors and breast lesions are easier to heat, it is suggested that heating limitation may be the reason for the lack of enhanced effects of combined treatment for large tumors and nonbreast lesions.

The other randomized trials including an international trial for breast cancer [30], a European Society for Hyperthermic Oncology (ESHO) trial for malignant melanoma [31], a Japanese Society for Therapeutic Radiology and Oncology (JASTRO) trial for superficial tumors [32] have clearly demonstrated the improvement of local control rate with the use of hyperthermia. Additionally, no enhancement of normal tissue damages by radiation was found. Thus, clinical benefits of hyperthermia combined with radiotherapy appear established for superficial tumors.

IV. Clinical Applications to Deep-Seated Tumors

Site-specific trials have been undertaken. A summary of those trials is shown in Table I.

A. Trials for Esophageal Cancers

Using an RF intracavitary heating device, Sugimachi *et al.*have applied hyperthermia in combination with radiotherapy and chemotherapy to patients with esophageal carcinoma. The long-term results were compared between two groups of patients treated with hyperthermo-chemo radiotherapy (HCRT) and those with chemo radiotherapy (CRT). The five-year survival rates of patients with respectable carcinoma, given preoperative HCRT or CRT, were 43.2% and 14.7%, respectively ($p < 0.05$). The two-year survival rates of those with unresectable carcinoma and receiving HCRT or CRT were 15.5% and 1.2%, respectively [33]. A prospective randomized trial was carried out to examine the effects of hyperthermia given preoperatively. Sixty-six patients with esophageal cancer underwent subtotal esophagectomy following either preoperative HCRT or CRT therapy. The incidence of lack of viable cancer cells in the resected specimens was 25% in the HCRT group and 5.9% in the CRT group. The cumulative three-year survival rate was 50.4% in the HCRT group and 24.2% in the CRT group [34].

B. Trials for Lung Cancers

It has been shown that RF capacitive heating devices can effectively raise temperatures of invasive lung tumors that were in

TABLE I
SUMMARY OF CLINICAL REPORTS FOR DEEP-SEATED TUMORS

A. Esophageal Cancer

Authors	Tumor type	No. of patients	Heating methods	Combined treatment	Survival rate
Kuwano M et al.1993	resectable tumor	183	intraluminal RF capacitive	chemoradiotherapy	5Y 43.2%
	unresectable tumor	114	intraluminal RF capacitive	chemoradiotherapy	2Y 15.5%
Kitamura K et al.1995	resectable tumor	66	intraluminal RF capacitive	chemoradiotherapy	3Y 24.2%

B. Lung Cancer

Authors	No. of patients	Heating methods	Combined treatment	Response rate (CR + PR)	Complication
Hiraoka M et al.1992	20	RF capacitive	radiotherapy	75% (17%+58%)	pain,dyspnea
Karasawa K et al.1994	19	RF capacitive	radiotherapy	95% (26%+69%)	

C. Liver Cancer

Authors	Tumor type	No. of patients	Heating methods	Combined treatment	Response rate (CR + PR)	Survival rate	Complication
Nagata Y et al.1997	HCC	73	RF capacitive	chemoradiotherapy	31% (10%+21%)	1Y 30% 5Y 17.5%	local pain
	non-HCC	45	RF capacitive	chemoradiotherapy	45% (7%+38%)	1Y 32.5%	
Kondo M et al.1993	metastatic tuomor from colorectal cancer	14	RF capacitive or Total body hyperthermia	chemotherapy	57%	Median 23months	pain,fever
Tanaka K et al.1992	HCC	18	RF capacitive	Intra-arterial chemotherapy (DSM)	56%		fever,epigastralgia mostly related to embolization
Yumoto Y et al.1991	HCC	20	RF capacitive	Intra-arterial chemotherapy (TAE)	40%		fever,pain, myelosupression

HCC : Hepatocellular carcinoma DSM : degradable starch microspheres TAE : transarterial embolization

D. Gastric Cancer

Authors	Tumor type	No. of patients	Heating methods	Combined treatment	Response rate (CR + PR)	Survival rate
Hamazoe R et al.1991	peritoneal dissemination	11	continuous hyperthermic peritoneal perfusion	chemotherapy	better than chemotherapy alone	
Kakehi M et al. 1990	gastric cancer	33	RF capacitive	chemotherapy	39% (9%+30%)	
Nagata Y et al.1995	inoperable gastric cancer	21	RF capacitive	chemotherapy	89%	1Y 39.1%

contact with the chest walls. We reported clinical results of 20 patients with lung cancer treated by thermoradiotherapy [35]. The mean of $T_{\max}$, T_{ave}, and $T_{\min}$ was 42.9 °C, 41.6 °C, and 39.7 °C, respectively. Of 12 tumors treated by a curative intent, two (17%) achieved complete response (CR), seven (58%) partial response (PR), and three (25%) no change (NC). The side effects associated with hyperthermia were pain in 12 patients (60%) and dyspnea in three (15%), all of which resolved after termination of treatment.

Improvement of local response rate [36] and survival rate [37] has been demonstrated with the combined treatment of regional hyperthermia and radiation therapy in nonrandomized trials.

TABLE I *(Continued.)*
SUMMARY OF CLINICAL REPORTS FOR DEEP-SEATED TUMORS

E. Colorectal Cancer

Authors	Tumor type	No. of patients	Heating methods	Combined treatment	Response rate (CR + PR)	Survival rate	Complication
Nishimura Y et al.1995	recurrent colorectal cancer	71	RF capacitive	radioherapy	54%		ileus,fistula
Ohno S et al. 1997	resectable tumor	88	intracavitary hyperthermia	chemoradiotherapy		5Y 91.3%	

F. Urinary Bladder Cancer

Authors	Tumor type	No. of patients	Heating methods	Combined treatment	Response rate (CR + PR)
Masunaga S et al.1994	resectable tumor	49	RF capacitive	radiotherapy	83% (Tave.>41.5℃)

G. Soft Tissue Tumors

Authors	Tumor type	No. of patients	Heating methods	Combined treatment	Response rate (CR + PR)	Survival rate 5Year
Hiraoka M et al.1995	unresectable tumor	31	RF capacitive	Chemoradiotherapy	74% (42%+32%)	5Y 48%

C. Trials for Liver Tumors

Heating capability of the 8-MHz RF capacitive device was evaluated for 77 liver tumors. The maximum tumor temperature, average tumor temperature, and minimum tumor temperature in the hepato cellular carcinoma (HCC) were (mean ± standard error) 41.2±0.2 °C, 40.3±1.3 °C, and 40.1±0.2 °C, respectively. The same thermometry results for non-HCC were 42.3±0.2 °C, 41.2±0.2 °C, and 40.9±0.2 °C, respectively. The maximum and minimum temperatures (41.8± 0.2 °C and 40.3±0.4 °C) in the patients with a CR or PR were higher than those in the patients with no response (NR) or progressive disease (PD) (41.2±0.5 °C and 39.8±0.4 °C), but the difference was not significant.

Of the 73 cases with HCC who were evaluated by CT, CR was achieved in 7 (10%), PR in 15 (21%), NR in 37 (51%), and PD in 14 (19%).

Of the 45 cases involving liver metastases evaluated by CT, CR was achieved in 3 (7%), PR in 17 (38%), NR in 12 (27%), and PD in 13 (29%). The one-year cumulative survival rate for HCC patients was 30.0%, and the five-year survival rate was 17.5%. The one-year survival of non-HCC patients was 32.5%, and the longest survival was 30 months. The sequelae of hyperthermia included focal fat necrosis in 20 patients (12%), gastric ulceration in four (2%), and liver necrosis in one (1%). The sequelae of thermometry were severe peritoneal pain in seven patients, intraperitoneal hematoma in one, and pneumothorax in one [38].

A number of strategies have been proposed that might lead to an selective heating of tumors. One of these is a manipulation of blood flow by degradable starch microspheres (DSMs). A DSM is a cross-linked starch microsphere with a mean diameter of 45 μm. It is dissolved by a α-amylase in the serum with a biological half-life of 15–30 min. Blood flow in tumors is shown to decrease transiently, leading to an increase in heating when DSM is administered in a feeding artery of tumors during hyperthermia. The accelerated increase in the liver temperature in accordance with the administration of DSM in the common hepatic artery during regional hyperthermia has been demonstrated in an experiment using pigs [39]. A clinical trial showed that transarterial embolization (TAE) with DSM helped 0.9 °C increase in the maximum tumor temperature [40].

The usefulness of combined treatment of intra-arterial chemotherapy and hyperthermia have been suggested in several clinical reports [41].

Complications were mostly related to the chemoembolization with DSM, which included fever, epigastric pain, and so on [38].

The clinical benefit of combined treatment of hyperthermia and TAE has been demonstrated in a randomized trial. Twenty patients were randomly assigned to either hyperthermia plus TAE or TAE alone. Regional hyperthermia was administered at tumor temperatures of more than 42.5 °C for 40 min twice a week, to a total of 10–38 sessions. The response rate was 40% in the ten patients treated by hyperthermia plus TAE and 20% in the ten patients treated by TAE alone. The patients treated by hyperthermia plus TAE had a tendency to have better survival rates than those of the TAE group. The main side effects of TAE plus hyperthermia were low-grade fever, localized pain, myelosupression, and liver dysfunction, but these were transient and eventually resolved [42].

D. Trials for Gastric Cancers

The heating capability of Thermotron RF-8 for peritoneally disseminated tumors from gastric or colorectal tumors was investigated. Tumor temperatures were measured by thin Teflon-coated microthermocouples, which had been implanted under laparotomy or inserted transcutaneouly under ultrasonography

into the center of the tumors. Of six tumors heated, tumor temperature could be raised over 43 °C in one tumor, 42 °C–43 °C in one tumor, and less than 42 °C in the remaining four tumors [43].

Hyperthermia in combination with chemotherapy was applied to 33 patients with gastric cancer. Hyperthermia was regionally given twice a week to a total of 6–40 sessions using an 8-MHz RF capacitive heating device. Chemotherapy consisted of mitomycin C (MMC) and 5-FU derivatives. Of the 33 patients treated, three (9%) showed CR and ten (30%) PR [41].

Recurrent and/or inoperable gastric cancer has been treated by thermoradiotherapy at Kyoto University Hospital, Kyoto, Japan, since 1983. The local response rate (complete regression plus partial regression/all tumors) was 88.9%, which seemed to be higher than that of other reports using thermochemotherapy or radiotherapy alone. The one-year cumulative survival rate was 39.1% [44].

E. Trials for Colorectal Cancers

The efficacy of RF capacitive heating is high for pelvic tumors, especially for large recurrent colorectal cancers.

We have treated 71 patients with unresectable or locally recurrent colorectal cancer by radiotherapy with or without locoregional hyperthermia [45]. Thirty-five patients were treated by radiotherapy plus hyperthermia (group I), while 36 patients were treated by radiotherapy alone (group II), mainly because of difficulties with the insertion of temperature probes or the thickness of the patients subcutaneous fat. The total radiation dose did not differ between groups I and II, but the mean tumor volume was significantly larger in group I than in group II. The incidence of freedom from local tumor regression at six months after the treatment was 59% (17/29) and 37% (11/30) for group I and group II, respectively. The objective response rate (CR + PR) was 54% (19/35) in group I, whereas it was 36% (10/28) in group II. A higher response rate of 67% was obtained in the 15 tumors with a T_{ave} of more than 42 °C compared with 47% for 17 tumors with a T_{ave} of less than or equal to 42 °C, although this difference was not significant. The incidences of obstructive ileus and intestinal fistula were relatively higher in group I (20%, 8.5%) than in group II (3%, 0%).

The usefulness of RF intracavitary hyperthermia combined with chemotherapy and radiotherapy as a preoperative treatment for rectal cancer has been investigated [46]. Postoperative prognoses were compared among 36 patients with carcinoma of the rectum, who were given preoperative HCR therapy followed by surgery, and 52 patients undergoing surgery alone without any preoperative therapy. There were significant differences in the prognosis between patients given preoperative HCR therapy plus surgery and those having surgery alone, and five-year survival rates were 91.3% and 64%, respectively. Particularly for patients with tumors invading beyond the muscularis propria and/or with positive lymph node metastasis, a significantly longer survival was obtained with HCR plus surgery than in surgery alone (86.5% versus 50.9% and 92.9% versus 51.7%, respectively). However, no significant differences were observed in the postoperative prognosis for cases with no lymph-node metastasis and/or with tumors limited to the muscularis propria between these two groups.

F. Trials for Urinary Bladder Cancers

Most trials for urinary bladder cancers were undertaken with the use of RF capacitive heating devices.

Preoperative radiotherapy or thermoradiotherapy was administered to 49 patients with bladder cancer. Twenty-eight patients were treated by radiation therapy combined with hyperthermia (group I). Radiation therapy was delivered with 4-Gy per fraction, 3 fractions per week to a total dose of 24 Gy ($\mathrm{TDF} = 53$). The other 21 patients were treated by the same radiation therapy regimen without hyperthermia (group II). Regional hyperthermia was administered for 35–60 min immediately after irradiation (two sessions per week to a total of four sessions) using an 8-MHz RF capacitive heating device. Group I was divided into group I (High), in which the average intravesical temperature (T_{ave}) was above 41.5 °C (12 patients), and group I (Low) with a T_{ave} below 41.5 °C (16 patients). The incidence of down-staging for group I (High), group I (Low) and group II was 83%, 38%, and 48%, and that of tumor degeneration was 83%, 44%, and 40%, respectively. The differences in response rate between group I (High) and the other groups were significant ($p < 0.05$). Survival rate tended to be higher in the group I than in the group II. This trend is more apparent for those cases with T3–4 or Grade-3 bladder cancer for which preoperative treatment is considered to be more indicated [47].

G. Trials for Soft Tissue Tumors

We have treated 31 unresectable and/or recurrent soft tissue tumors in 27 patients by hyperthermia in combination with radiation therapy. Tumor volume ranged from 3 to 3927 cm^3, with a mean of 428 cm^3. Locoregional hyperthermia was delivered once or twice a week for 40–60 min to a total of 2–14 sessions. Radiation therapy was given at doses of 20.8–70 Gy. The mean of $T_{\max}$, T_{ave}, $T_{\min}$ was, respectively, 44.0 °C, 42.3 °C, and 40.1 °C. Of the 31 tumors treated, 13 (42%) showed CR, 10 (32%) PR, and 8 (26%) NC. Of 20 tumors in which the early response to thermoradiotherapy was assessed by X-CT, massive intratumoral low-density areas reflecting coagulation necrosis by hyperthermia was shown in six (30%) tumors. All of these tumors demonstrated a marked response on follow-up or histopathological examinations. Thermal parameters were more influential than the total irradiation dose in terms of both tumor regression and the appearance of intratumoral low-density areas. The five-year survival of 18 patients who had no distant metastases at the start of treatment was 48% [48].

V. Conclusion

Technical and clinical aspects for hyperthermia techniques used in Japan have been reviewed in this paper. Several methods of improving the heating characteristics from the various heating device have been proposed. Regional heating can be efficiently achieved by using RF capacitive techniques. That is because regional heating techniques apply energy to

the adjacent deep-seated tumors in an unfocused manner and energy is also delivered to the adjacent normal tissue. This condition makes it possible to realize selective heating of tumors when heat dissipation by blood flows more predominant than in normal tissue. A double-electrode capacitive applicator has been proposed to attain deep heating locally.

To avoid fat tissue heating, inductive heating is effective. However, the eddy current has a tendency of distributing near the surface of the human body due to its inherent nature. As a result, hot spots arise near the surface of the human body. To prevent this phenomena, the eddy current was controlled by introducing an auxiliary electrode and eddy-current absorber.

When using hyperthermia, it is important to establish accurate local and deep-heating techniques and to be able measure the temperature distribution throughout the heated volume. To attain this goal, a wireless thermometer with an implant function was proposed, although this is an invasive method. A future goal is to use MRI and spectroscopic techniques for noninvasive mapping of the temperature distribution.

Many clinical trials have been introduced with detailed investigation of the response rate.

Nonrandomized trials undertaken in Japan for locally advanced breast cancers, esophageal cancers, lung cancers, liver tumors, gastric cancers, unresectable, or recurrent colorectal cancers and invasive urinary bladder cancers demonstrated higher response rate in thermoradiotherapy than in radiotherapy alone. Randomized trials have been carried out for esophageal cancers and gastric cancers, and both of them showed improved local response with the combined use of hyperthermia. Additionally, the complications associated with treatment were not generally serious, except for chronic bowel damages suggested in a trial for colorectal cancers. These clinical results indicate the benefit of combined treatment of hyperthermia and radiotherapy for various malignancies.

The use of heat in cancer therapy is the subject of an ever-broadening multidisciplinary research effort involving the fields of biology, physics, engineering, and medicine. There are many questions still to be answered regarding biological issues such as thermotolerance and thermal dose. Major efforts should be devoted to the development of a device that is capable of raising the whole tumor volume to therapeutic temperatures without overheating the adjacent normal tissues. With the advancement of these technologies, hyperthermia will be more widely and safely used in the treatment of cancers.

REFERENCES

[1] M. Abe and M. Hiraoka, "Review; Localized hyperthermia and radiation in cancer therapy," *Int. J. Radiat. Biol.*, vol. 47, no. 4, pp. 347–359, Apr. 1985.

[2] C. Streffer, P. Vaupel, and G. M. Hahn, *Biological Basis of Oncologic Thermotherapy*. Berlin, Germany: Springer-Verlag, 1990.

[3] S. Mizusina, "Non-inductive thermometry," in *Proc. 6th Int. Congr. Hyperthermia Oncol.*, vol. 2, 1992, pp. 45–51.

[4] K. Kuroda, "Non-invasive temperature imaging by MR system," in *Proc. 8th Int. Congr. Hyperthermia Oncol.*, May 2000, p. 119.

[5] C. A. Perez *et al.*, "Clinical results of irradiation combined with local hyperthermia," *Cancer*, vol. 52, no. 9, pp. 1597–1603, Nov. 1983.

[6] Y. Nikawa *et al.*, "Development and testing of a 2450 MHz lens applicator for localized microwave hyperthermia," *IEEE Trans. Microwave Theory Tech.*, vol. MTT-33, pp. 1212–1216, 1985.

[7] Y. Nikawa *et al.*, "Heating system with a lens applicator for 430 MHz microwave," *Int. J. Hyperthermia*, vol. 6, no. 3, pp. 671–684, May–June 1990.

[8] T. Matsuda *et al.*, "Heating characteristics of a 430 MHz microwave heating system with a lens applicator," *Int. J. Hyperthermia*, vol. 6, pp. 685–696, 1990.

[9] M. D. Sapozink, F. A. Gibbs, K. S. Gates, and J. R. Stewart, "Regional hyperthermia in the treatment of clinically advanced, deep seated malignancy: Results of a pilot study employing an annular array applicator," *Int. J. Radiat. Oncol. Biol. Phys.*, vol. 10, no. 6, pp. 775–786, June 1984.

[10] M. Abe *et al.*, "Multi-institutional studies on hyperthermia using an 8 MHz radiofrequency capacitive heating device (Thermotron RF8) in combination with radiation for cancer therapy," *Cancer*, vol. 58, no. 8, pp. 1589–1595, Oct. 1986.

[11] H. Kato, T. Fukuhara, and I. Yamamoto, "Capacitive-type heating.," in *Cancer Treatment by Hyperthermia, Radiation and Drugs*, T. Matsuda, Ed. New York: Taylor & Francis, 1993, pp. 23–36.

[12] C. W. Song, J. G. Rhee, C. K. K. Lee, and S. H. Levitt, "Capacitive heating of phantom and human tumors with an 8 MHz radiofrequency applicator (Thermotron RF- 8)," *Int. J. Radiat. Oncol. Biol. Phys.*, vol. 12, no. 3, pp. 365–372, Mar. 1986.

[13] M. Hiraoka *et al.*, "Radiofrequency capacitive hyperthermia for deep-seated tumors. I. Studies on thermometry," *Cancer*, vol. 60, no. 1, pp. 121–127, Jul. 1987.

[14] Y. Kotsuka and E. Hankui, "Investigation on two types of applicators for local hyperthermia of induction and capacitive heating," in *Proc. Int. EMC Symp.*, vol. 2, Sept. 1989, pp. 722–725.

[15] H. Kato *et al.*, "A new inductive applicator for hyperthemia," *J. Microwave Power*, vol. 18, pp. 331–335, 1983.

[16] H. Kato *et al.*, "Heating characteristic of inductive aperture-type applicator," *Jpn. Hypertherm. Oncol.*, vol. 2, no. 1, pp. 3–12, Mar. 1986.

[17] S. Kuroda *et al.*, "Thermal distribution of radiofrequency inductive hyperthermia using an inductive aperture-type applicator: evaluation of the effect of tumor size and depth," *Med. Biol. Eng. Comput.*, vol. 37, pp. 285–290, 1999.

[18] Y. Kotsuka, E. Hankui, and Y. Shigematsu, "Development of ferrite core applicator system for deep-induction hyperthemia," *IEEE Trans. Microwave Theory Tech.*, vol. 44, pp. 1803–1810, Oct. 1996.

[19] Y. Kotsuka *et al.*, "Investigation of heating region for new magnetic induction heating system for treating breast hyperthermia," in *Proc. Asia–Pacific Microwave Conf.*, Dec. 1998, pp. 1291–1295.

[20] K. Sugimachi *et al.*, "Endotract antenna for application of hyperthermia to malignant lesions.," *Jpn. J. Cancer Res.*, vol. 74, no. 5, pp. 622–624, Oct. 1983.

[21] L. Hamada, H. Yoshimura, and K. Ito, "A new heating technique for temperature distribution control in interstitial microwave hyperthermia," *IEICE Trans. Electron.*, vol. E82-C, no. 7, pp. 1318–1325, July 1999.

[22] K. Saito, O. Nakayama, L. Hamada, and K. Ito, "Analysis of temperature distributions generated by square array applicator composed of coaxial-slot antennas for hyperthermia," *Trans. IEICE*, vol. 1, J82-B, no. 9, pp. 1730–1738, Sept. 1999.

[23] L. Hamada, H. Yoshimura, and K. Ito, "Dielectric-loaded coaxial-slot antenna for interstitial microwave hyperthermia: Longitudinal control of heating patterns," *Int. J. Hyperthermia*, vol. 16, no. 3, pp. 219–229, June 2000.

[24] T. Kobayashi, "Interstitial hyperthermia of malignant brain tumors and oral cancers by implant heating system (IHS)," in *Hyperthermic Oncology*, E. W. Gerner, Ed. Tuscon, AZ: Arizona Board of Regents, 1992, vol. 389.

[25] I. Tohnai, Y. Goto, Y. Hayashi, M. Ueda, T. Kobayashi, and M. Matsui, "Preoperative thermochemotherapy of oral cancer using magnetic induction hyperthermia (implant heating system: IHS)," *Int. J. Hyperthermia*, vol. 12, no. 1, pp. 37–47, Jan.–Feb. 1996.

[26] Y. Kotsuka, K. Orii, H. Kojima, K. Kamogawa, and M. Tanaka, "New wireless-thermometer for RF and microwave thermal therapy using an MMIC in an Si BJT VCO Type," *IEEE Trans. Microwave Theory Tech.*, vol. 47, pp. 2630–2635, Dec. 1999.

[27] J. Overgaard, "The current and potential role of hyperthermia in radiotherapy," *Int. J. Radiat. Oncol. Biol. Phys.*, vol. 16, pp. 535–549, 1989.

[28] C. A. Perez, T. Pajak, and B. Emami *et al.*, "Randomized phase III study comparing irradiation and hyperthermia with irradiation alone in superficial measurable tumors," Radiation Therapy Oncol. Group. Amer. J. Clin. Oncol., Final Rep., vol. 14, 1991.

[29] N. Takeshita, Y. Tanaka, and T. Matsuda, "Evaluation of CT images, tumor response and prognosis after thermodadiotherapy for deep-seated tumors," *Int. J. Hyperthermia*, vol. 9, no. 1, pp. 1–17, 1993.
[30] C. C. Vernon, J. W. Hand, S. B. Field, D. Machin, J. B. Whaley, J. van der Zee, W. L. van Putten, G. C. van Rhoon, J. D. van Dijk, D. Gonzalez, F. F. Liu, P. Goodman, and M. Sherar, "Radiotherapy with or without hyperthermia in the treatment of superficial localized breast cancer: Results from five randomized controlled trials. International collaborative hyperthermia group," *Int. J. Radiat. Oncol. Biol. Phys.*, vol. 35, no. 4, pp. 731–744, Jul. 1, 1996.
[31] J. Overgaard, Gonzalez, D. Gonzalez, M. C. Hulshof, G. Arcangeli, O. Dahl, O. Mella, and S. M. Bentzen, "Hyperthermia as an adjuvant to radiation therapy of recurrent or metastatic malignant melanoma. A multicentre randomized trial by the European Society for Hyperthermic Oncology," *Int. J. Hyperthermia*, vol. 12, no. 1, pp. 3–20, Jan.–Feb. 1996.
[32] JASTRO Study Group, , "A randomized phase III trial of hyperthermia in combination with radiotherapy for superficial tumors," *J. Jpn. Soc. Theraput. Radiol. Oncol.*, vol. 10, pp. 161–164, 1998.
[33] H. Kuwano, H. Matsuura, and M. Mori, "Hyperthermia combined with chemotherapy and irradiation for the treatment of patients with carcinoma of the oesophagus and the rectum," in *Cancer Treatment by Hyperthermia, Radiation and Drugs*, T. Matsuda, Ed. New York: Taylor & Francis, 1993, pp. 353–364.
[34] K. Kitamura *et al.*, "Prospective randomized study of hyperthermia combined with chemoradiotherapy for esophageal carcinoma," *J. Surg. Oncol.*, vol. 60, no. 1, pp. 55–58, Sept. 1995.
[35] M. Hiraoka *et al.*, "Regional hyperthermia combined with radiotherapy in the treatment of lung cancers," *Int. J. Radiat. Oncol. Biol. Phys.*, vol. 22, no. 5, pp. 1009–1014, 1992.
[36] H. Terashima *et al.*, "Pancoast tumour treated with combined radiotherapy and hyperthermia—A preliminary study," *Int. J. Hyperthermia*, vol. 7, no. 3, pp. 417–424, May–Jun. 1991.
[37] K. Karasawa *et al.*, "Thermoradiotherapy in the treatment of locally advanced nonsmall cell lung cancer," *Int. J. Radiat. Oncol. Biol. Phys.*, vol. 30, no. 5, pp. 1171–1177, Dec. 1, 1994.
[38] Y. Nagata *et al.*, "Clinical results of radiofrequency hyperthermia for malignant liver tumors," *Int. J. Radiat. Oncol. Biol. Phys.*, vol. 38, no. 2, pp. 359–365, May 1997.
[39] K. Akuta *et al.*, "Regional hyperthermia combined with blockade of the hepatic arterial blood flow by degradable starch microspheres in pigs.," *Int. J. Radiat. Oncol. Biol. Phys.*, vol. 13, no. 2, pp. 239–242, Feb. 1987.
[40] Y. Tanaka *et al.*, "Effects of multimodal treatment and hyperthermia on hepatic tumors," *Cancer Chemother. Pharmacol.*, vol. 31, pp. S111–S114, 1992.
[41] M. Kondo, H. Oyamada, and T. Yoshikawa, "Therapeutic effects of chemoembolization using degradable starch microspheres and regional hyperthermia on unresectable hepatocellular carcinoma," in *Cancer Treatment by Hyperthermia, Radiation and Drugs*, T. Matsuda, Ed. New York: Taylor & Francis, 1993, pp. 317–327.
[42] Y. Yumoto *et al.*, "Trans-catheter hepatic arterial injection of lipiodol soluble anti-cancer agent SMANCS and ADR suspension in lipiodol combined with arterial embolization and local hyperthermia for treatment of hepatocellular carcinoma," *Int. J. Hyperthermia*, vol. 7, no. 1, pp. 7–17, 1991.
[43] R. Hamazoe *et al.*, "Heating efficiency of radiofrequency capacitive hyperthermia for treatment of deep-seated tumors in the peritoneal cavity," *J. Surg. Oncol.*, vol. 48, no. 3, pp. 176–179, Nov. 1991.
[44] Y. Nagata *et al.*, "Clinical experiences in the thermoradiotherapy for advanced gastric cancer," *Int. J. Hyperthermia.*, vol. 11, no. 4, pp. 501–510, Jul.–Aug. 1995.
[45] Y. Nishimura *et al.*, "Hyperthermia combined with radiation therapy for primary unresectable and recurrent colorectal cancer," *Int. J. Radiat. Oncol. Biol. Phys.*, vol. 23, no. 4, pp. 759–768, 1992.
[46] S. Ohno *et al.*, "Improved surgical results after combining preoperative hyperthermia with chemotherapy and radiotherapy for patients with carcinoma of the rectum," *Disease Colon Rectum.*, vol. 40, no. 4, pp. 401–406, Apr. 1997.
[47] S. Masunaga *et al.*, "The phase I/II trial of preoperative thermoradiotherapy in the treatment of urinary bladder cancer," *Int. J. Hyperthermia*, vol. 10, pp. 31–40, 1994.
[48] M. Hiraoka, Y. Nishimura, S. Masunaga, M. Koishi, M. Mitsumori, Y. P. Li, Y. Nagata, K. Akuta, M. Takahashi, and M. Abe, "Clinical results of thermoradiotherapy of soft tissue tumors," *Int. J. Hyperthermia*, vol. 11, pp. 365–377, 1995.

Masahiro Hiraoka was born in Ehime Prefecture, Japan, in 1952. He graduated from Kyoto University, Kyoto, Japan, in 1977.

In 1995, he became Chairman and Professor of the Department of Therapeutic Radiology and Oncology, Graduate School of Medicine, Kyoto University. His subjects of interest include radiation oncology (especially breast cancer and gastrointestinal tumors), hyperthermic oncology, and development of integrated radiotherapy system. He has been involved with the development of various heating devices, including RF capacitive equipment, MW equipment, ultrasound equipment.

Michihide Mitsumori was born in Osaka Prefecture, Japan, in 1960. He graduated from Kyoto University, Kyoto, Japan, in 1985, and received the M.D. degree from Kyoto University, in 1994.

His subjects of interest include radiation oncology (especially breast cancer, prostate cancer, and esophageal cancer), clinical hyperthermia using RF and MW devices, and application of nanoparticles to hyperthermia.

Naotoshi Hiroi was born in Osaka, Japan, in 1965. He graduated from Fukui Medical University, Fukui, Japan, in 1991.

In 1996, he joined the Department of Therapeutic Radiology and Oncology, Graduate School of Medicine, Kyoto University, Kyoto, Japan, where he is involved in research dealing with the clinical effect by brachytherapy and hyperthermia. He has authored and co-authored six papers in the field of chemoradiation and clinical hyperthermia.

Shinji Ohno was born in Fukuoka, Japan, in 1958. He received the Medical License degree in 1984, and the Ph.D. degree from Kyushu University, Fukuoka, Japan, in 1992.

From 1989 to 1991, he joined the Division of Hematology and Oncology, Texas Medical School, Houston, TX, where he was involved in research dealing with the effects of whole body hyperthermia combined with chemotherapy. He has authored and co-authored 80 papers in the field of oncology. He is with the Department of Surgery II, Kyushu University, where he is especially involved with carcinoma of the esophagus, colon and breast.

Yoshiaki Tanaka was born in 1941. He received the Medical License degree from the Ministry of Health and Welfare, Nagoya, Japan, in 1967, and the Dr. Med. Science degree from the Nagoya University Postgraduate School, Nagoya, Japan, in 1971.

From 1974 to 1977, he was an Assistant Professor in the Department of Radiology, Nagoya University Hospital. From 1977 to 1978, he was Research Fellow in the Cancer Research and Treatment Center, University of New Mexico. From 1985 to 1993, he was Chief Director in the Department of Therapeutic Radiology, Tokyo Metropolitan Komagome Hospital. He is currently a Professor and Chairman in the Department of Radiology, Nihon University School of Medicine, Tokyo, Japan.

Dr. Tanaka is a Board Certified Fellow of the Japanese Society for Therapeutic Radiology and Oncology of the Japanese Society for Therapeutic Radiology and Oncology.

Youji Kotsuka (M'74–SM'99) was born in Kanagawa, Japan, on April 30, 1941. He received the Dr.Eng. degree from the Tokyo Institute of Technology, Tokyo, Japan, in 1980.

In 1974, he was a Lecturer at Tokai University, Tokyo, Japan, and is currently a Professor of telecommunication engineering. From 1995 to 1996, he was a Visiting Professor at the Harvard University, Cambridge, MA. He has been involved with the development of RF dielectric and inductive applicators for deep hyperthemia, the development of EM-wave absorbers using ferrites, shield techniques, EM theory on scattering from random rough surfaces, and propagation in anisotropic media with losses. He was Chair of the Medical Application and Measurement Techniques Committee with Radiated Waves for the Institute of Electrical Engineering, Japan.

Dr. Kotsuka is a member of the Steering Committee of the IEEE Microwave Theory and Techniques Society (IEEE MTT-S), Tokyo Chapter, and a member of National Commissions A and K of the URSI.

Keizo Sugimachi was born in Nagasaki Prefecture, Japan, in 1938. He graduated from Kyushu University, Fukuoka, Japan, in 1963.

In 1985, he became Chairman and Professor in the Department of Surgery II, Kyushu University. His subjects of interest include surgical oncology (especially esophageal cancer and gastric cancer), liver diseases (especially liver cancer, portal hypertension, and liver transplantation), and endoscopic surgery. He has been an editor and co-editor of many journals in the field of surgery. Since 1997, he has been the Chief Director of the Japan Society of Cancer Therapy. He was President of 99th Japan Surgical Society in 1999.

DNA AND CELL BIOLOGY
Volume 21, Number 2, 2002

Pp. 81–90

Cloning of the Chicken Immunoglobulin Joining (J)-Chain Gene and Characterization of its Promoter Region

TOMIHISA TAKAHASHI,[1] MASAYO KIMURA,[1]
NAOYUKI MATSUMOTO,[1] ARIHIRO IWATA,[1] YOSHITAKA OGURA,[1] TOSHIYUKI YOSHIDA,[1]
NOBUHIRO KAMEI,[1] KAZUO KOMIYAMA,[1] JIRI MESTECKY,[2] and ITARU MORO[1]

ABSTRACT

Three overlapping genomic clones of the chicken immunoglobulin joining (J) chain were isolated and then characterized using restriction enzyme analysis, Southern blot analysis with cDNA probes, and DNA sequencing. The gene consisted of four exons separated by a 2.6-kb intron 1, a 0.9-kb intron 2, and a 0.5-kb intron 3. A transcriptional initiation site was identified by a primer extension method using mRNA and cDNA, indicating that exon 1 was 86 bp encoding 20 amino acid residues. A TATA box was positioned at 29~25 bp upstream of exon 1. Exons, 2, and 3 consisted of 133 bp and 81 bp, encoding 43 and 26 amino acid residues of the mature protein, respectively. Exon 4 consisted of 202 bp encoding 66 amino acid residues and 1.2 kb of untranslated sequence. Deletion mutants of a 4.1-kb genomic fragment containing exon 1 showed high levels of promoter activities when examined in luciferase reporter assays following transfection into the DT-40 chicken B-cell line. These results suggest that the chicken J-chain gene consists of four exons and three introns and that the transcriptional regulatory elements may be present within 3.8 kb upstream of exon 1.

INTRODUCTION

THE IMMUNOGLOBULIN JOINING (J) CHAIN is an acidic polypeptide with a molecular mass of 15 kDa covalently linked by disulfide bonds to polymeric Igs such as dimeric and tetrameric IgA and pentameric IgM. It plays important roles in polymerization and secretion of these polymeric Igs (Koshland, 1985; Mestecky and McGhee, 1985). Furthermore, it has been demonstrated that IgA- and IgM-producing cells as well as IgG and IgD myeloma cells express J chains (Brandtzaeg, 1974; Kaji and Parkhouse, 1974). Other studies have reported the presence of IgM polymer without the J chain in cells and serum (Randall *et al.*, 1990; Brewer *et al.*, 1994), leaving questions concerning its specific functions. However, the presence of J chain results in secretion of pentameric IgM instead of hexameric IgM and is required for correct assembly of dimeric IgA (Koshland, 1989; Randall *et al.*, 1992). The selective transport of polymeric IgA and pentameric IgM through the mucosal epithelial cells is mediated by the polymeric Ig receptor (pIgR), and the J chain is necessary for pIgR to recognize pIgs (Brandtzaeg, 1985).

The structural analyses of human and mouse J-chain genes have revealed that both consist of four exons and three introns and span more than 7 kb (Max and Korsmeyer, 1985; Matsuuchi *et al.*, 1986). However, the expression patterns of the J chain genes in B cells differ between the human and mouse (Koshland, 1985; Max and Korsmeyer, 1985). Studies of human B-cell lines representing various developmental stages have demonstrated that J-chain expression is found in pro-B and pre-B cells at an early stage of development before synthesis of Ig (Max and Korsmeyer, 1985; Mestecky *et al.*, 1997). In contrast, murine J chain is detectable in late-stage, mature B cells expressing cytoplasmic μ chain but not in B cells expressing surface μ chain (Koshland, 1985). Although this discrepancy has not been clarified, the differential expression of J chain in the human and mouse could be the result of evolutionary divergence. However, it is considered that the constitutive expression of J chain is closely related to the induction and synthesis of H- and L-chains of Igs.

The transcriptional mechanisms of the murine J-chain gene have been investigated. An early study demonstrated that the

[1]Department of Pathology, Nihon University School of Dentistry, Tokyo, Japan.
[2]Department of Microbiology, The University of Alabama at Birmingham, Birmingham, Alabama.

T-cell cytokines interleukin (IL)-2 and IL-5 are important factors for upregulating J-chain expression in mature B-cell lines (Matsui *et al.*, 1989; McFadden and Koshland, 1991). Functional analysis of the 5′-flanking region of the murine J-chain gene revealed three regulatory elements and their nuclear factors (Lansford *et al.*, 1992). The nuclear factors PU. 1 (Shin and Koshland, 1993) and B-MEF2 (Rao *et al.*, 1998), which are members of the Ets-related protein and myocyte enhancer families, are activators of the murine J-chain gene. On the other hand, the B-cell-specific activator protein BSAP, which is a member of the Pax family, is a repressive factor for the J-chain gene (Rikenberger *et al.*, 1996). Furthermore, the fourth regulatory element, which is an upstream stimulatory factor (USF), has been shown to be a positive regulator of murine J-chain transcription (Wallin *et al.*, 1999).

Nucleotide sequences of cDNA encoding the J chain have revealed that mammalian J chains including human (Max and Korsmeyer, 1985), cow (Kulseth and Rogne, 1994), mouse (Cann *et al.*, 1982), and possum (Adamski and Demmer, 1999) display highly conserved features. In avian species, comparative studies have reported that chicken Igs such as IgA and IgM are analogous to those of mammals and that J chain purified from serum IgM is cross-reactive with an anti-human J-chain antibody (Kobayashi and Hirai, 1980). In addition, cDNA cloning of the chicken J chain has demonstrated that the deduced amino acid sequence, consisting of 158 residues, has a high degree of homology with those of mammals and that its mRNA expression is found in various tissues such as spleen, intestine, Harderian gland, and bursa of Fabricius (Takahashi *et al.*, 2000). An ontogenic study using embryonic bursa of Fabricius also has demonstrated that chicken J-chain expression is initiated during the same period as that of surface IgM during B-cell development (Takahashi *et al.*, 2000). However, the regulatory mechanisms of the chicken J-chain gene have not been clarified. In order to understand the regulatory mechanisms of chicken J-chain transcription, we isolated a chicken genomic clone including the 5′-flanking region and characterized the promoter activity. Promoter activities within 4.1 kb of the 5′-flanking region containing exon 1 were measured by transient transfection experiments using the chicken B-cell line DT-40, showing the location of some sequences important for transcriptional activity.

MATERIALS AND METHODS

Screening of genomic library

An EMBL 3 SP6/T7 genomic library (Clontech, Palo Alto, CA, USA) prepared from chicken liver was screened by plaque hybridization using a random-primed ^{32}P-labeled 1.0-kb fragment (CHJ-1), which encodes an ORF of chicken J-chain cDNA (Takahashi *et al.*, 2000), as the probes. Approximately 6×10^6 genomic clones were hybridized with the probe in a buffer containing 50% formamide, 4× SSC, 50 mM HEPES, pH 7.0; 10× Denhardt's solution, and heat-denatured salmon sperm DNA at 42°C for 16 h. After hybridization, filters were washed three times for 30 min in 0.2× SSC/0.1% SDS at 60°C. Positive clones were selected for further screening. Moreover, a 0.1-kb fragment (J-1) containing the initiation codon (ATG) was synthesized by PCR using primers 5′-GCAAGATGAAGACCTC-3′ (sense) and 5′-AGCACACGCTCCTCAC-3′ (antisense) designed from the chicken J-chain cDNA sequence (Takahashi *et al.*, 2000). Three positive clones were amplified, and DNA was extracted using a λ DNA kit (Qiagen, Hilden, Germany) and then digested with appropriate restriction enzymes for subcloning into the vector pBluescript (pBS) SK(-).

RNA extraction and primer extension analysis

Total RNA was extracted from adult chicken spleen using the acid guanidinium thiocyanate method (Chomczynski and Sacchi, 1987). mRNA was purified using an oligo(dT) column (Oligotex™-dT30 Super; Roche Molecular Biochemical, Mannheim, Germany) according to the manufacturer's instructions. An oligonucleotide primer (pET-2: 5′-GACTTCTTC-CTCAGGATTGTCTTTGGAGGGGAC-3′) was synthesized according to the complementary nucleotide sequence of chicken J-chain cDNA (Takahashi *et al.*, 2000). Primer extension analysis was performed as described in a previous report (Boorstein and Craig, 1989). Appropriate amounts (1, 5, 10 μg) of mRNA isolated from adult chicken spleen were hybridized with [γ-^{32}P]-end-labeled pET-2 in a buffer containing 100 mM Tris HCl, pH 8.3; 100 mM KCl, 20 mM $MgCl_2$, 20 mM DTT, 2 mM dNTPs, and 1 mM spermidine at 58°C for 20 min. The extension reaction was performed using 5 U of avian myeloblastosis virus RT (Promega, Madison, WI, USA) at 42°C for 30 min. The extension products were separated on a 6% acrylamide sequencing gel with sequencing products generated by pET-2 on a chicken J-chain cDNA clone, CHJ-2 (Takahashi *et al.*, 2000), as molecular size markers and then visualized by autoradiography.

Cell culture

The chicken B-cell line DT-40, which expresses surface IgM (Uckun *et al.*, 1996), was purchased from Human Science Research Resources Bank (Osaka, Japan) and maintained prior to transfection in 100-mm tissue culture dishes (Iwaki Glass, Tokyo) containing RPMI 1640 medium supplemented with penicillin (100 U/ml), streptomycin (10 μg/ml), and 20% heat-inactivated chicken serum at 37°C in a humidified incubator in an atmosphere containing 5 % CO_2 before transfection.

Reporter plasmids

Luciferase reporter plasmid vectors, pGL3-Control, pGL3-Basic, and pSV-β-Galactosidase Control were purchased from Promega.

DNA sequencing

Nucleotide sequences were determined using a Thermo Sequenase II dye terminator cycle sequence kit (Amersham Pharmacia Biotech, Buckinghamshire, UK) and a Mega Base 1000™ (Molecular Dynamics, Sunnyvale, CA, USA) according to the manufacturer's instructions with T7 and M13 reverse primers or with sequence-specific oligonucleotide primers. DNA sequences obtained were analyzed using computer software Genetyx Mac Ver. 10.1 (Software Development Co., Tokyo).

Preparation of deletion mutants

A 4.1-kb *Xho*I/*Hin*dIII fragment from a genomic clone containing exon 1 of the chicken J chain was subcloned into the *Xho*I/*Hin*dIII site of pGL3-Basic. Then a series of 5′ deletion mutants were prepared using the Erase-a-base system (Promega) according to the manufacturer's instructions. The plasmid was linearized by digestion with *Kpn*I, and then Exonuclease III digestion was performed at 37°C and terminated at 30-sec intervals. The precise deletion endpoints and base substitutions were determined by sequence analysis, as described above.

Transient transfection and reporter gene assay

Transient trasfectants were prepared using electroporation. The DT-40 cells were washed with PBS (-) and adjusted to 5×10^5 cells/ml with 500 μl of HEPES-buffered saline in a Gene Pulser Cuvette (0.4-cm electrode gap; Bio-Rad Laboratories, Hercules, CA, USA). Then 10 μg of reporter plasmid DNA was added to the cell suspension, and electroporation was carried out at 250 V, 960 μF for 35 msec using the Gene Pulser®II (Bio-Rad). After washing with serum-free medium, cells were cultured with fresh complete medium containing 20% chicken serum for 48 h at 37°C in a humidified incubator in an atmosphere containing 5% CO_2, then harvested for reporter gene assays.

Luciferase and β-galactosidase assays were performed using the Dual-Luciferase® Reporter Assay System (Promega) according to the manufacturer's instructions. Values of luciferase activity detected by test reporter plasmid were adjusted for variation in transfection efficiency by dividing by values obtained for β-galactosidase activity in the same culture dishes.

RESULTS

Isolation and restriction map of chicken J-chain gene

Screening of the chicken genomic library using CHJ-1 (Takahashi *et al.*, 2000) as the probe resulted in two positive clones, pGJ-1 and pGJ-2, containing inserts of 19.2 kb and 16.5 kb, respectively. Southern blot analysis revealed that both clones lacked completely the upstream sequence including exon 1 and intron 1. Thus, further screening was performed using the PCR product J-1 as the probe, resulting in the identification of pGJ-3 containing an insert of 12.8 kb that overlapped several restriction sites in pGJ-1 and pGJ-2. The restriction map of the chicken J-chain gene (Fig. 1) was derived by combination the digestion patterns of pGJ-1, -2 and −3. Several fragments were isolated by digestions with restriction enzymes and subcloned into pBSSK(-).

Sequence analysis demonstrated that the chicken J-chain cDNA (Takahashi *et al.*, 2000) was derived from four exons in the genomic DNA and that the exon–intron organization was consistent with the human (Max and Korsmeyer, 1985) and mouse (Matsuuchi *et al.*, 1986) genes. Exon 1 was found to have a structure typical of the eukaryocytic leader exon reported for the murine J chain (Matsuuchi *et al.*, 1986) and was composed of 86 bp, including 25 bp of untranslated sequence at the 5′ end and 61 bp encoding a leader sequence for the J-chain protein. Exons 2 and 3 were composed of 133 and 81 bp encoding 69 amino acids and including the N-terminus of the mature J-chain protein. Exon 4 was composed of 202 bp, encoding the remaining 66 amino acids at the C-terminus and the termination codon plus 1.2 kb of 3′ untranslated sequence (Fig. 2). As shown in Figure 2 and Table 1, the four exons are separated by three introns of various sizes (2.6, 0.9, and 0.5 kb) and have typical splicing signals at the exon–intron boundaries.

Mapping of the transcription-initiation site and comparison of the 5′-flanking region

The transcription-initiation site of the chicken J chain was determined by primer extension analysis using a ^{32}P-labeled oligonucleotide primer (pET-2) complementary to the sense strand of the cDNA. The primer was annealed to appropriate amounts of mRNA isolated from adult chicken spleen and extended using RT. As shown in Figure 3A, analysis of extension products on a sequencing gel revealed a product of 200 bp, indicating that the transcription-initiation site was located 25 bases upstream of the start codon (ATG) of chicken J-chain cDNA. These data indicated that, in contrast to the mouse promoter, the chicken J-chain promoter has a single transcription-initiation site.

A highly conserved feature of the nucleotide sequence of the 5′-flanking region of J chain genes has been reported for mouse (Matsuuchi *et al.*, 1986) and bovine sequences (Kulseth and Rogne, 1994). Therefore, the sequence upstream of the chicken

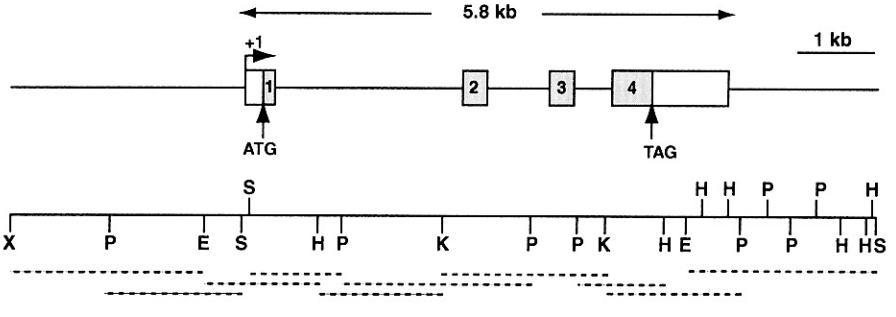

FIG. 1. Structure of the chicken J-chain gene. The top and middle lines represent the gene with a partial restriction map. The shadowed boxes represent exons 1 through 4, and the open boxes represent the 5′ and 3′ UTRs. The dotted lines at the bottom indicate subclones generated for the DNA sequencing. E = *Eco*RI; H = *Hin*dIII; K-*Kpn*I; P = *Pst*I; S = *Sac*I; X = *Xho*I.

FIG. 2. Selected DNA sequences from the chicken J-chain gene. Amino acid sequences encoded by the four exons are shown under their corresponding codons. The TATA box is underlined, and the transcription initiation site is marked by an asterisk. The boundaries of exons and introns are indicated by lowercase letters. The sequence has been deposited in EMBL, GenBank, and DDJB under Accession No. AB076374.

J-chain gene was aligned with the mouse and bovine sequences. As shown Figure 3B, a TATA box motif was identified at 29~25 bp upstream of the transcription-initiation site of the chicken J-chain gene, identical to the mammalian sequences. In addition, a well-conserved sequence (ATCATTTGCACAC) was observed at the 5′ end of the TATA box. Significant sequences in the 5′-flanking region of the murine J chain, JA and JB, were identified as a positive regulatory motif and an IL-2-responsive element (Lansford *et al.*, 1992), respectively. Although present in the bovine, these sequences are not conserved in the chicken.

Promoter activity of the 5′-flanking region of the chicken J-chain gene

The promoter activity of the 5′-flanking region of the chicken J-chain gene was examined by transient transfection assay in the chicken B-cell line DT-40 using the luciferase gene as a re-

TABLE 1. COMPARISON OF THE STRUCTURE OF HUMAN, MOUSE, AND CHICKEN J-CHAIN GENES

Gene segment	Length (kb)			Homology (%)	
	Chicken	Mouse	Human	Human	Mouse
Exon 1	0.086	0.064	ND[a]	ND[a]	50
Exon 2	0.133	0.121	0.122	62	61
Exon 3	0.081	0.081	0.081	78	75
Exon 4	0.202	0.211	0.208	50	50
Intron 1	2.650	1.370	ND[a]	I[b]	
Intron 2	0.907	3.700	4.500	I	
Intron 3	0.489	0.900	0.670	I	
3′ UTR	1.210	0.709	0.787	I	

[a]Exon 1 and intron 1 are omitted because data are not available for these segment of the human J chain.
[b]I = insignificant.

porter, along with the pSV-β-Galactosidase Control plasmid. Various fragments comprising a series of deletions in the 5′-flanking region were subcloned into the pGL3-Basic vector (Fig. 4A). As shown in Figure 4B, luciferase activities were determined for the mutants 3757pGL, 3129pGL, 2817pGL, 2215pGL, 1797pGL, 1262pGL, 851pGL, and 170pGL, containing the 5′-flanking region with the TATA box and exon 1; and high levels of activity were detected. However, low luciferase activity was found for a deletion mutant +265pGL, which lacked the upstream sequence including the TATA box and exon 1. Furthermore, mutant 3757pGL3 had approximately 20-fold higher luciferase activity than mutant +265pGL3, indicating that the upstream sequences including exon 1 play significant roles in the regulation of chicken J-chain gene expression.

DISCUSSION

To study the molecular basis of transcriptional regulation of the chicken J-chain gene, we isolated a chicken genomic J-chain fragment (7.8 kb) composed of four exons, three introns, and 3.1 kb of 5′-flanking region from the first exon, including the leader sequence. No differences were found in the exon–intron organization of the human (Max and Korsmeyer, 1985), mouse (Matsuuchi *et al.*, 1986), and chicken J-chain genes. The nucleotide sequences of the four exons in the chicken have a high degree of homology with those of the human and mouse, suggesting that these species have diverged with few mutation or other changes in the coding regions.

It has been shown that an octamer sequence (ATTTGCAT) is located upstream of the transcription-initiation site of the murine J-chain gene (Koshland, 1985; Sigvardsson *et al.*, 1993) and that the same motif is found in the promoter region of Vκ and Vλ gene segments in Igs of the human and mouse (Falkner and Zachau, 1984; Parslow *et al.*, 1984). Our results indicate that an octamer sequence is located 54 bp upstream of the transcription-initiation site of the chicken J-chain gene and is highly conserved with those of the murine and bovine J-chain genes (Fig. 3). Gene transfer experiments have shown that this octamer sequence is a recognition site for two distinct octamer binding factors, Oct-1 and Oct-2. These are members of the POU family in vertebrates (Staudt et al., 1986; Petryniak *et al.*, 1986) and are required for the correct initiation of Ig gene transcription, contributing to lymphocyte-specific expression (Falkner and Zachau, 1984; Parslow *et al.*, 1984; Staudt *et al.*, 1986; Petryniak *et al.*, 1990; Foster *et al.*, 1985). These data suggest that murine J-chain expression is controlled through signaling pathways similar to those controlling the transcriptional activity of the L-chain gene. In chickens, an octamer sequence that can interact with Oct-1 and Oct-2 derived from nuclear extracts of chicken B cells has been found in the promoter region of the Vλ gene segment and shown to mediate transcriptional activity for gene rearrangement (Petryniak *et al.*, 1990). Therefore, the chicken J chain and L-chain genes appear to share the octamer elements involved in initiating transcription and in coordinating the expression of these molecules, as is seen in the mouse.

It has been established that IL-2 and IL-5 can upregulate murine J-chain expression in mature B-cell lines (Matsui *et al.*, 1989; McFadden and Koshland, 1991). Analysis of promoter activity has indicated that two distinct sequences, JA and JB, are present in the 5′-flanking region of the murine J-chain gene (Fig. 3B). The JB element, which plays a central role in murine J-chain gene expression following IL-2-stimulation (Lansford *et al.*, 1992), is fully conserved between the mouse and cow (Kulseth and Rogne, 1994) but not in chicken, as shown in this study. The JA element contains both positive and negative regulatory motifs that act as repressors in J-chain-nonexpressing cells and as an activator in J-chain-expressing cells (Lansford et al., 1992). However, neither JB nor JA sequences are conserved in the chicken (Fig. 3B). Furthermore, studies of the mouse have shown that the JB element comprises 5 nucleotides that interact with transcription factor PU.1 (Shin and Koshland, 1993) and that the JA motif is composed of 8 nucleotides that interact with B-MEF (Rao *et al.*, 1998). Our results demonstrated that a putative binding site for Ets-1, a member of the Ets protein family (Bosselut *et al.*, 1990) including PU.1, is located 1157 bp upstream of the transcription-initiation site of the chicken J-chain gene (Fig. 5). However, there were no motifs homologous to JB and JA in the 4.1-kb upstream sequence, suggesting that the transcriptional mechanism of the chicken J-chain gene may not be associated with IL-2-stimulation, unlike the murine J-chain gene.

Functional analysis of the 5′-flanking region of the chicken J-chain gene suggested that two important elements were located at -170 to +265 and −3757 to −3129 (Fig. 4). We consider that a fragment positioned at -170 to +265 and containing the TATA box is the promoter region and the sequence at −3757 to −3129 is part of an enhancer region. In the promoter region, some transcription factor-binding sites, such as for NF-AT and AP-4, have been predicted by TRUNSFAC analysis (Wingender *et al.*, 2001). The NF-AT is a transcription factor that binds to a sequence in the IL-2 promoter (Shaw *et al.*, 1988) and can induce 3′ enhancer activity of the Ig κ chain, associated with both Jun and Fos in B cells activated by phorbol 12-myristate 13-acetate (PMA) and ionomycin (Meyer and Ireland, 1998). On the other hand, AP-4 is a transcription factor in the group of basic helix–loop-helix (bHLH) proteins that is expressed ubiquitously and binds the E-box elements of the hu-

A

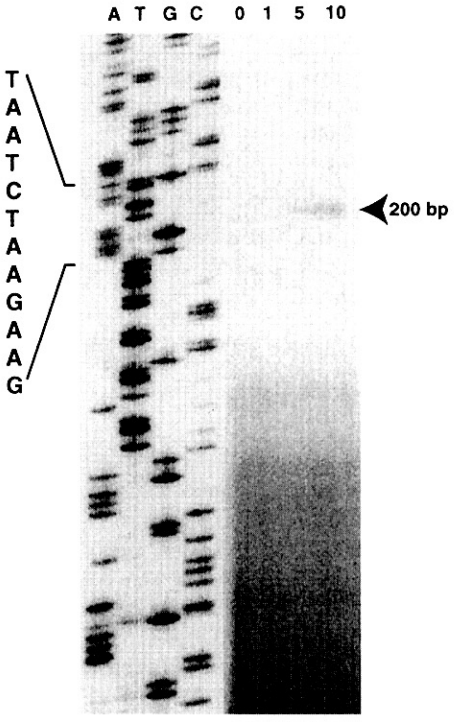

B

```
      -154
Ch    ACTGG-TTTCAGTCCCCTAGCCACATTTTCCAGTGTCAGAGCTAGCCAGCTGGGCTGTTT
Co    CTAAA-TTGCAGAGTTCAA-CCGCAGTTGTGA---TCTTAGTTTGTTAGCTGCCTGGAGT
Mo    CCAGAGTAGCATGCAGTTGAAACCTGAAGCTGTGATGACTGCAGCTCACCTGTCCTGGGG
            *  **             *                *     *       * ***    *

      -95      JA      JB
Ch    ATTCTTAGGAAACAACATAAGTG-TATCATTTGCACACAGCCTTATAGG-CAGGCACATG
Co    GTTATTTTTAAGAAAGCAGAAGCCCCATCATTTGCACACT-CCTTATAGCTCACACACCTT
Mo    TTATTTTTTAAGAAAGCAGAAGCAGCATCATTTGCACACC-TCTTATAGA-CACACACAGT
       *   **    * *  *  **  ***     **************    *******   **   ***

      -13                   +1
Ch    CTCTCC----------ACTCACATTCTTCAAAAGAAGGGAAGGCGAGATG
Co    AACCCTGACTTCTTAGCTCCAGTTTTTCAAAAGAAGTGAAGTCAAGATG
Mo    TGGCCGTGGCTTTTGGCTTCAGTCTTTCAACA---GTGAAGACAAGATG
            *              **     *  *****  *   * **** * *****
```

FIG. 3. Primer extension of the transcription initiation site of the chicken J-chain gene and alignment of the 5′-flanking regions. **(A)** A primer was applied to appropriate amounts (1, 5, 10 μg) of mRNA extracted from spleen. The primer extension product is indicated by an arrow; ATGC = size markers corresponding to a chicken J-chain cDNA (Takahashi *et al.*, 2000). **(B)** Alignments of approximately 150 bp of 5′-flanking regions of the J-chain genes of mouse (Mo; Matsuuchi *et al.*, 1986), cow (Co; Kulseth and Rogne, 1994), and chicken (Ch). Nucleotide numbers are indicated at left, representing the first base in the transcriptional start codon (ATG). An open box indicates well-conserved sequence; a double underline indicates the TATA box; underlines indicate a positive regulatory motif (JA) and an IL-2-responsive element (JB) reported in the murine J-chain sequence (Koshland, 1985; Lansford *et al.*, 1992). Identical nucleotides are indicated by asterisks.

man and murine Ig κ promoters, indicating important and novel roles for transcriptional regulation of Ig synthesis (Aranburu *et al.*, 2001). Considering that transcription of both the chicken and murine J-chains is closely linked to that of Ig, these lines of evidence suggest the possibility that NF-AT and AP-4 have a significant effect in inducing the promoter activity of the chicken J-chain gene and that PMA and ionomycin are necessary to activate chicken J-chain transcription.

The most important sequence involved in the chicken J-chain gene transcription seems to be positioned from −3757 to −3129 bp. In the mouse, it has been reported that enhancer elements located 7.5 kb upstream of the J-chain gene interact with

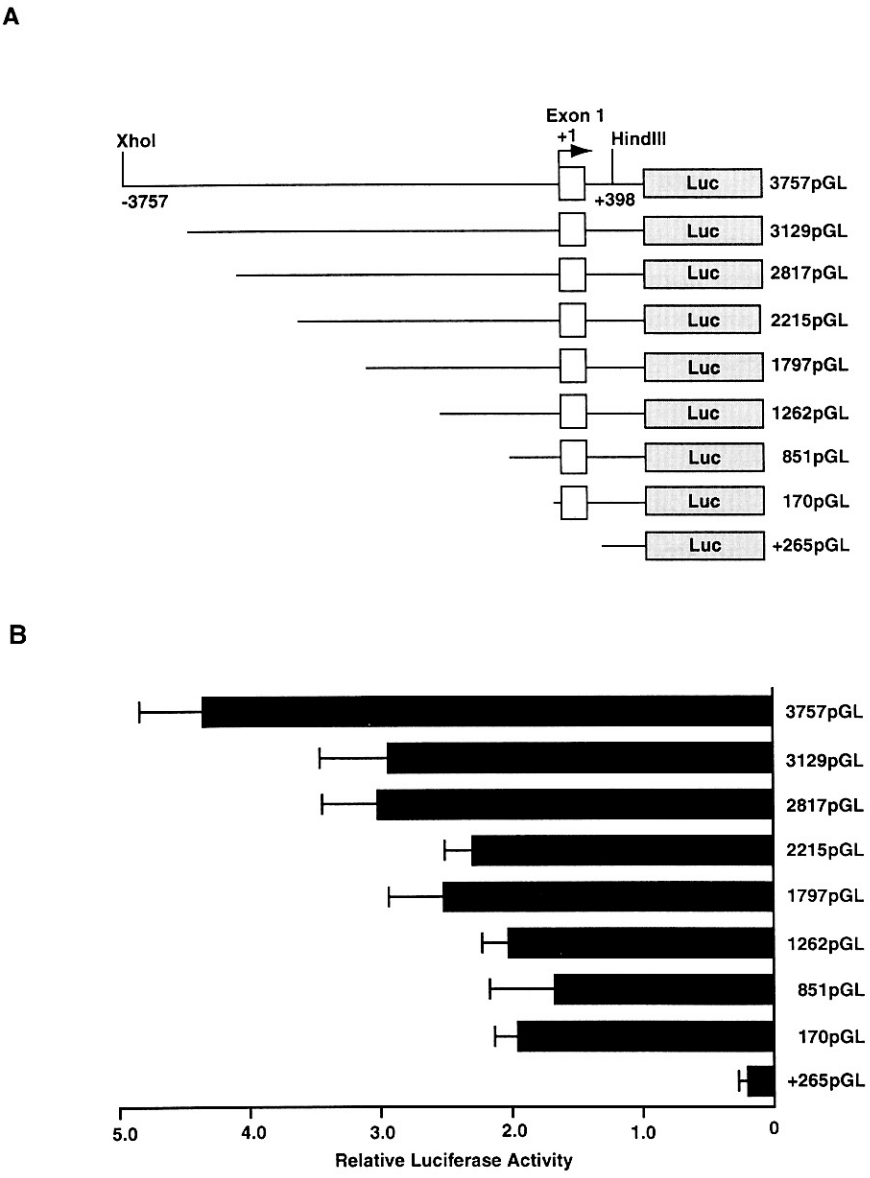

FIG. 4. Luciferase activity of fragments upstream of chicken J-chain gene. **(A)** Construction of deletion mutants in pGL3-basic. A 4.1-kb fragment was subcloned into the *Xho*I and *Hin*dIII sites of pGL3-basic. The upstream fragments containing exon 1 have their 5′ ends at −3757, -3129, -2817, -2215, -1797, -1262, -851, and −170, as indicated. The +265pGL3 construct does not contain exon 1 (+265 to +398). **(B)** Each deletion mutant (10 μg) was cotransfected with pSV-β-galactosidase control vector into DT-40. After 48 h, luciferase and β-galactosidase activities were measured. The results were calculated as relative luciferase activity by dividing by the values for β-galactosidase activity. Results for each group represent the mean of three experiments.

the transcription factor STAT-5 in B cells activated by IL-2 stimulation (Kang *et al.*, 1998). Our sequence data did not reveal a STAT-5-binding site within this 3.8 kb. However, some fragments may have important roles in the transcription of the chicken J-chain gene. Indeed, we found ubiquitous nuclear factor binding sites such as for NF-E2, cMyb, MyoD, TCF11, NF-AT, and USF located within −3757 to −3129 bp (Fig. 5). The fragment encompassing approximately 500 bp upstream of the 5′ end had the highest level of luciferase activity of all the deletion mutants and contained a variety of binding sites for transcription factors such as cMyb, MyoD, NF-AT, and USF-1. In particular, USF-1, a member of the bHLH transcription factor family (Rao *et al.*, 1997), has binding activity to the consensus sequence of E-box elements and positively regulates transcription of the murine J-chain gene (Wallin *et al.*, 1999). Furthermore, μ heavy chain-enhancer activity has been detected in the presence of three protein–DNA complexes comprising Ets-1 and bHLH transcription factors, such as USF-1, PU.1 and TFE3 (Rao *et al.*, 1997). Considering that expression of the chicken J chain is closely related to that of μ heavy chain, there is the

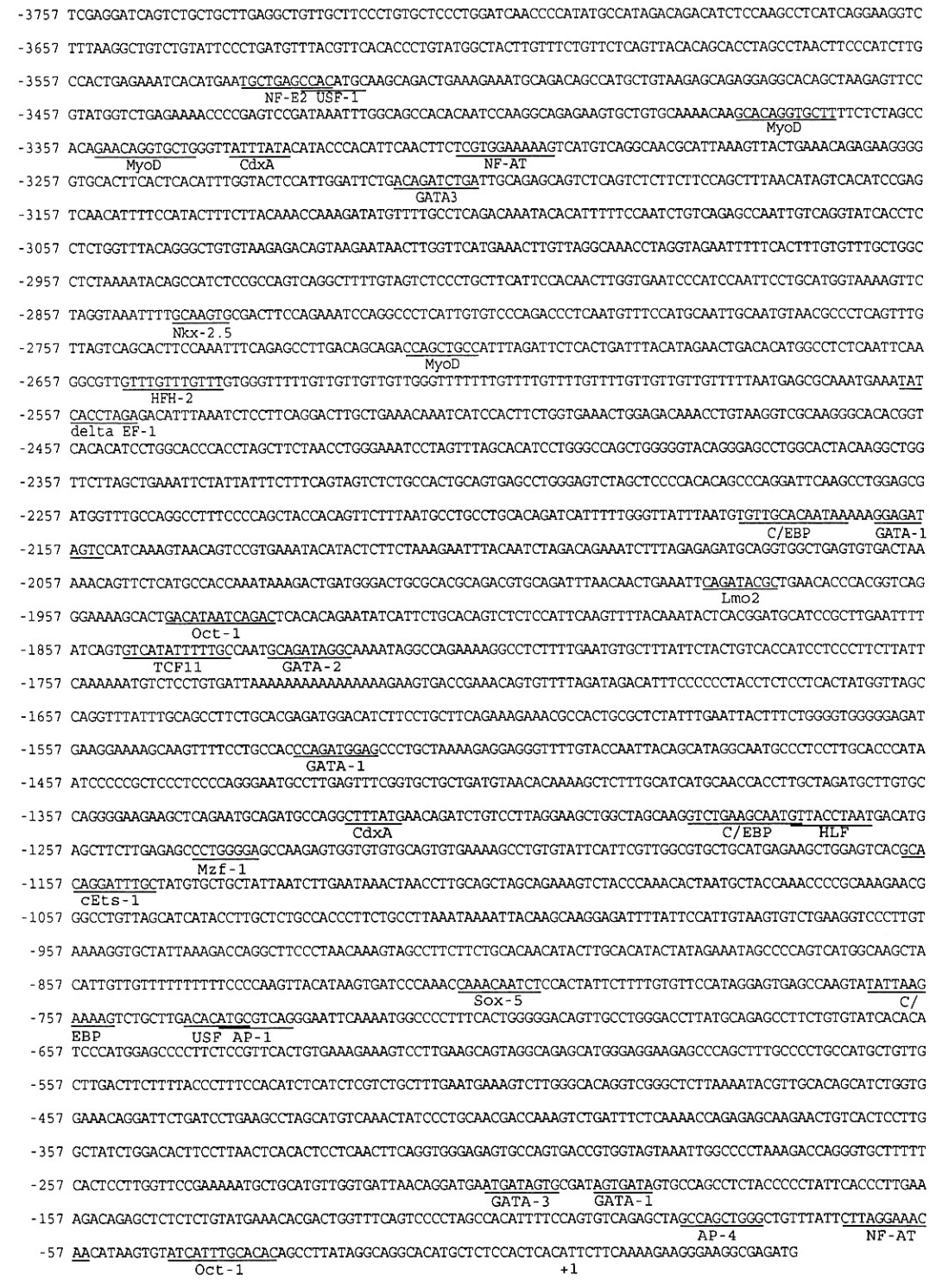

FIG. 5. Nucleotide sequence of the 5′ flanking region of the chicken J-chain gene. The transcription initiation site is at +1. Transcription factor binding sites of interest, determined using the TRANSFAC program, are underlined and labeled. The Accession No. is AB076375.

possibility that its transcription would be dependent on the interaction of Ets-1 and bHLH transcription factors.

Several studies of the murine J chain have demonstrated that some factors, such as PU.1 (Shin and Koshland, 1993), BSAP (Rikenberger *et al.*, 1996), B-MEP2 (Rao *et al.*, 1998), and USF-1 (Wallin *et al.*, 1999), have the ability to bind to consensus motifs identified in a chromatin hypersensitive site spanning the 5′-flanking region. On the other hand, TRANSFAC analysis of a 3.8-kb fragment of the chicken J chain indicated several motifs, such as Oct-1 (Staudt *et al.*, 1986), NF-AT

(Shaw *et al.*, 1988), USF-1 (Rao *et al.*, 1997), and AP-4 (Meyer and Ireland, 1998) binding sites, which may be related to B-cell activation. However, it is unclear whether chicken analogs of these transcription factors are involved in regulation of J-chain gene expression, compatible with B-cell activation. Further detailed studies are required to understand the regulation of the chicken J-chain gene, including purification, characterization, and functional studies of these sequences.

ACKNOWLEDGMENTS

This work was supported by a Grant-in-Aid for Scientific Research (No. 11307043) from the Ministry of Education, Culture, Sports, Science and Technology, Japan, Nihon University Research Grant for Assistants, and in a part of the Sato Fund from Nihon University School of Dentistry.

REFERENCES

ADAMSKI, F.M., and DEMMER, J. (1999). Two stages of increased IgA transfer during lactation in the marsupial, *Trichosurus vulpecula* (Brushtail possum) J. Immunol. **162,** 6009–6015.

ARANBURU, A., CARLSSON R., PERSSON C., and LEANDERSON, T. (2001). Transcription factor AP-4 is a ligand for immunoglobulin-κ promoter E-box elements. Biochem. J. **354,** 431–438.

BOORSTEIN, W.R., and CRAIG, E.A. (1989). Primer extension analysis of RNA. Methods Enzymol. **180,** 347–369.

BOSSELUT, R., DUVALL, J.F., GÉGONNE, A., BAILLY, M., HÉMAR, A., BRADY, J., and GHYSDAEL, J. (1990). The product of the *c-ets*-1 proto-oncogene and the related Ets2 protein act as transcriptional activators of the long terminal repeat of human T cell leukemia virus HTLV-1. EMBO J. **9,** 3137–3144.

BRANDTZAEG, P. (1974) Presence of J chain in human immunocytes containing various immunoglobulin classes. Nature **252,** 418-420.

BRANDTZAEG, P. (1985) Role of J chain and secretory component in receptor-mediated glandular and hepatic transport of immunoglobulins in man. Scand. J. Immunol., **22,** 111-146.

BREWER, J.W., RANDALL, T.D., PARKHOUSE, R.M.E., and CORLEY, R.B. (1994). IgM hexamers? Immunol. Today **15,** 165–168.

CANN, G..M., ZARITSKY, A., and KOSHLAND, M.E. (1982). Primary structure of the immunoglobulin J chain from the mouse. Proc. Natl. Acad. Sci. USA **79,** 6656–6660.

CHOMCZYNSKI, P., and SACCHI, N. (1987). Single-step method of RNA isolation by guanidium thiocyanate–phenol-chloroform extraction. Anal. Biochem. **162,** 156–159.

FALKNER, F.G., and ZACHAU, H.G. (1984). Correct transcription of an immunoglobulin κ gene required an upstream fragment containing conserved sequence elements. Nature **310,** 71–74.

FOSTER, J., STAFFORD, J., and QUEEN, C. (1985) An immunoglobulin promoter displays cell-type specificity independently of the enhancer. Nature **315,** 423–425.

KAJI, H., and PARKHOUSE, R.M.E. (1974). Intracellular J chain in mouse plasmacytomas secreting IgA, IgM, and IgG. Nature **249,** 45–47.

KANG, C.J., SHERIDAN, C., and KOSHLAND, M.E. (1998). A stage-specific enhancer of immunoglobulin J chain gene is induced by interleukin-2 in a presecretor B cell stage. Immunity **8,** 285–295.

KOBAYASHI, K., and HIRAI, H. (1980). Studies on the subunit components of chicken polymeric immunoglobulins. J. Immunol. **124,** 1695–1740.

KOSHLAND, M.E. (1985). The coming age of the immunoglobulin J chain. Annu. Rev. Immunol. **3,** 425–453.

KOSHLAND, M.E. (1989). The immunoglobulin helper: The J chain. In: *Immunoglobulin Gene XVII.* T. Honjo, F. W. Alt, and T. H. Rabbitts, eds. (Academic Press, London) pp. 345–359.

KULSETH, M.A., and ROGNE, S. (1994). Cloning and characterization of bovine immunoglobulin J chain cDNA and its promoter region. DNA Cell Biol. **13,** 37–42.

LANSFORD, R.D., McFADDEN, H.J., SIU, S.T., COX, J.S., CANN, G.M., and KOSHLAND M.E. (1992). A promoter element that exerts positive and negative control of the interleukin 2-responsive J-chain gene. Proc. Natl. Acad. Sci. USA **89,** 5966–5970.

MATSUI, K., NAKANISHI, K., COHEN, D.I., HADA, T., FURUYAMA, J., HAMAOKA, T. and HIGASHINO, K. (1989). B cell response pathways regulated by IL-5 and IL-2: Secretory μH chain-mRNA and J chain mRNA expression are separately controlled events. J. Immunol. **142,** 2918–2923.

MATSUUCHI, L., CANN, G.M., and KOSHLAND, M.E. (1986). Immunoglobulin J chain gene from the mouse. Proc. Natl. Acad. Sci. USA **83,** 456–460.

MAX, E.E., and KORSMEYER, S.J. (1985). Human J chain gene: structure and expression in B lymphoid cells. J. Exp. Med. **161,** 832–849.

McFADDEN, H.J., and KOSHLAND, M.E. (1991). Interleukin 2-and interleukin 5-induced changes in the binding of regulatory factors to the J-chain gene promoter. Proc. Natl. Acad. Sci. USA **88,** 11027–11031.

MESTECKY, J., and McGHEE, J.R. (1985). Immunoglobulin A (IgA): Molecular and cellular interactions involved in IgA biosynthesis and immune response. Adv. Immunol. **40,** 153–245.

MESTECKY, J., MORO, I., MOLDVEANU, Z., TAKAHASHI, T., IWASE, T., KUBAGAWA, H., and COOPER, M.D. (1997). Immunoglobulin J chain: An early differentiation marker of human B cells. Ann. NY Acad. Sci. **815,** 111–113.

MEYER, K.B., and IRELAND, J. (1998). PMA/ionomycin induces Igκ 3′ enhancer activity which is in part mediated by a unique NFAT transcription complex. Eur. J. Immunol. **28,** 1467–1480.

PARSLOW, T.G., BLAIR, D.L., MURPHY, W.J., and GRANNER, D.K. (1984). Structure of the 5′ ends of immunoglobulin genes: A novel conserved sequence. Proc. Natl. Acad. Sci. USA **81,** 2650–2654.

PETRYNIAK, B., STAUDT, L.M., POSTEMA, C.E., McCORMACK, W.T., and THOMPSON, C.B. (1990). Characterization of chicken octamer-binding proteins demonstrates that POU domain-containing homeobox transcription factors have been highly conserved during vertebrate evolution. Proc. Natl. Acad. Sci. USA **87,** 1099–1103.

RANDALL, T.D., KING, L.B., and CORLEY, R.B. (1990). The biological effects of IgM hexamer formation. Eur. J. Immunol. **20,** 1971–1979.

RANDALL, T.D., BREWER, J.W., and CORLEY, R.B. (1992). Direct evidence that J chain regulates the polymeric structure of IgM in antibody-secreting B cells. J. Biol. Chem. **267,** 18002–18007.

RAO, E., DANG, W., TIAN, G., and SEN, R. (1997), A three-protein–DNA complex on a B cell-specific domain of the immunoglobulin μ heavy chain gene enhancer. J. Biol. Chem. **272,** 6722–6732.

RAO, S., KARRY, S., GACKSTETTER, E.R., and KOSHLAND, M.E. (1998). Myocyte enhancer factor-related B-MEF 2 is developmentally expressed in B cells and regulates the immunoglobulin J chain promoter. J. Biol. Chem. **273,** 26123–26129.

RIKENBERGER, J.L., WALLIN, J.J., JOHNSON, K.W., and KOSHLAND, M.E. (1996). An interleukin-2 signal relieves BSAP (Pax-5)-mediated repression of immunoglobulin J chain gene. Immunity **5,** 377–386.

SIGVARDSSON, M., OLSSON, L., HôGBOM, E., and LEANDERSON, T. Characterization of the joining chain (J-Chain) promoter. (1993) Scand. J. Immunol., **38,** 411–416.

SHAW, J. P., UTZ, P. J., DURAND, D.B., TOOLE, J.J., EMMEL, E.A., and CRABTREE, G.R. (1988). Identification of putative regulator of early T cell activation genes. Science **241,** 202–205.

SHIN, M.K., and KOSHLAND, M.E. (1993) Ets-related protein PU.1 regulates expression of the immunoglobulin J-chain gene through a novel Ets-binding element. Genes Dev. **7,** 2006–2015.

STAUDT, L. M., SINGH, H., SEN, R., WIRTH, T., SHARP, P. A., and BALTIMORE, D. (1986). A lymphoid-specific protein binding to the octamer motif of immunoglobulin genes. Nature **323,** 640–643.

TAKAHASHI, T., IWASE, T., TACHIBANA, T., KOMIYAMA, K., KOBAYASHI, K., CHEN, C. H., MESTECKY, J., and MORO, I. (2000). Cloning and expression of the chicken immunoglobulin joining (J)-chain cDNA. Immunogenetics **51,** 85–91.

UCKUN, F.M., WADDICK, K.G., MAHAJAN, S., JUN, X., TAKATA, M., BOLEN, J. and KUROSAKI, T. (1996). BTK as a mediator of radiation-induced apoptosis in DT-40 lymphoma B cells. Science **273,** 1096–1100.

WALLIN, J.J., RINKENBERGER, J.L., RAO, S., GACKSTETTER, E.R., KOSHLAND, M.E., and ZWOLLO, P. (1999). B cell-specific activator protein prevents two activator factors from binding to the immunoglobulin *J chain* promoter until the antigen-driven stages of B cell development. J. Biol. Chem. **274,** 15959–15965.

WINGENDER, E., CHEN, X., FRICKE, E., GEFFERS, R., HEHL, R., LIEBICH, I., KRULL, M., MATYS, V., MICHAEL, H., OHNHAUSER, R., PRUSS, M., SCHACHERER, F., THIELE, S., and URBACH, S. (2001). The TRANSFAC system on gene expression regulation. Nucleic Acids Res. **29,** 281–283.

Address reprint requests to:
Dr. Tomihisa Takahashi
Department of Pathology
Nihon University School of Dentistry
1-8-13, Kanda-Surugadai, Chiyoda-ku
Tokyo 101-8310, Japan

E-mail: takahashi-tm@dent.nihon-u.ac.jp

Received for publication January 3, 2002; accepted January 7, 2002.

Immunogenetics (2002) 54:513–519
DOI 10.1007/s00251-002-0492-2

ORIGINAL PAPER

**Arihiro Iwata · Takashi Iwase · Yoshitaka Ogura
Tomihisa Takahashi · Naoyuki Matsumoto
Toshiyuki Yoshida · Nobuhiro Kamei
Kunihiko Kobayashi · Jiri Mestecky · Itaru Moro**

Cloning and expression of the turtle *(Trachemys scripta)* immunoglobulin joining (J)-chain cDNA

Received: 7 June 2002 / Accepted: 15 July 2002 / Published online: 6 September 2002

Abstract The J-chain protein is a M_r 15,000 polypeptide associated with polymeric IgA and IgM. The complete cDNA sequences of human, mouse, cow, brushtail possum, chicken and frog J chains have been previously reported, but nothing is known about the cDNA and amino acid sequences of reptilian J chain. Here, we determined a turtle J-chain cDNA sequence by RT-PCR and RACE, and examined J-chain mRNA and protein expression by Northern blotting and immunohistochemistry. This turtle J-chain cDNA was 1,934 bp and had an open reading frame of 477 nucleotides, encoding 159 amino acids. The mature J-chain protein is composed of 137 amino acids, M_r ~15,000. The deduced amino acid sequence of the turtle J chain was highly homologous to that of human (60%), mouse (61%), cow (60%), rabbit (60%), chicken (69%), brushtail possum (65%), *Rana catesbeiana* (47%) and *Xenopus laevis* (58%). Eight cysteine residues were located at the same positions as in these other species, with the exception of *X. laevis*. PROSITE database analysis indicated the presence of two N-glycosylation sites in turtle, one of which was novel. Northern blot analysis revealed that turtle J-chain mRNA was expressed in lung, stomach, spleen and intestine. In addition, immunohistochemistry showed J-chain-positive plasma cells in the intestine and spleen. These results suggest the presence of a mucosal immune system mainly composed of J-chain-containing Ig in the turtle.

Keywords Joining chain · Polymeric immunoglobulin · Phylogeny · Turtle · Immunohistochemistry

Turtle J-chain nucleotide sequence data are available in the DDBJ/EMBL/GenBank nucleotide sequence databases under the accession number AB085611

A. Iwata (✉) · T. Iwase · Y. Ogura · T. Takahashi · N. Matsumoto
T. Yoshida · N. Kamei · I. Moro
Department of Pathology, Nihon University School of Dentistry,
1-8-13, Kanda-Surugadai, Chiyoda-ku, Tokyo 101-8310, Japan
e-mail: iwata-a@dent.nihon-u.ac.jp
Tel.: +81-3-32198124, Fax: +81-3-32198340

K. Kobayashi
Department of Pediatrics, Hokkaido University School of Medicine,
Kita 15 Jyo-Nishi, Kita-ku, Sapporo 060-8638, Japan

J. Mestecky
Department of Microbiology, BBRB 757,
University of Alabama at Birmingham, Birmingham,
AL 35294, USA

Introduction

Mucosal surfaces are covered by a thin layer of vulnerable epithelium, which is continuously exposed to diverse pathogens such as bacteria and viruses, as well as various harmful molecules. An innate defense mechanism is present in these areas and a mucosal immune system composed of SIgA plays a crucial role in preventing invasion of foreign antigens (Mestecky and McGhee 1987). SIgA consists of dimeric (d) IgA and joining (J) chain, which are produced by plasma cells, and a polymeric immunoglobulin receptor (pIgR) that functions as a receptor for J-chain-containing polymeric immunoglobulins (Igs) (Mestecky and McGhee 1987).

The J chain is an acidic polypeptide of M_r 15,000 that has an important role in the polymerization and secretion of polymeric Igs (Brandtzaeg 1985; Brewer et al. 1994; Cattaneo and Neuberger 1987; Johansen et al. 2000; Mestecky et al. 1999; Mestecky and McGhee 1987). However, it has been reported that the J chain is present in IgG- and IgD-containing myeloma cells, as well as in IgA- and IgM-producing cells (Brandtzaeg 1974; Kaji and Parkhouse 1974; Mestecky et al. 1977). The presence of polymeric IgM without J chain in cells and serum has also been reported (Brewer et al. 1994; Kimura et al. 2001; Randall et al. 1990). In addition, polymeric IgM is secreted by a glioma cell line transfected with IgM heavy- and light-chain cDNA, even though this cell line does not produce J chain (Cattaneo and Neuberger 1987). The substitution of serine for cysteine in IgM, which is involved in J-chain binding, results in the formation of polymeric IgM without a J chain (Davis et al. 1989). The presence of J chain also results in the secre-

tion of pentameric IgM instead of hexameric IgM and is necessary for a correct assembly of dIgA (Koshland 1989; Randall et al. 1992). Other studies indicated that selective transport of dIgA and pentameric IgM through mucosal epithelial cells is mediated by the pIgR and that the J chain is necessary for pIgR to recognize pIgs (Brandtzaeg 1985). Therefore, the J chain is a key factor for the recognition of pIgs by pIgR localized in glandular epithelial cells.

The J-chain genes of human, mouse and chicken consist of four exons and three introns (Matsuuchi et al. 1986; Max and Korsmeyer 1985; Takahashi et al. 2002). However, the expression patterns of J-chain genes are different in these species. The J chain in humans is expressed in pro-B and pre-B cells at an early stage of development before synthesis of Ig (Max and Korsmeyer 1985; Mestecky et al. 1997). On the other hand, murine and chicken J chains are detectable in a late stage of mature B cells expressing cytoplasmic μ chain (Koshland 1985; Takahashi et al. 2000). It has been reported that J-chain mRNA expression ontogenetically occurs 1 week earlier than that of μ chain in the human fetal liver (Iwase et al. 1993). However, these discrepancies have not been clarified.

At present, full-length J-chain cDNA has been reported in mammals, birds and amphibia (Adamski and Demmer 1999; Hohman et al. 1997; Kulseth and Rogne 1994; Matsuuchi et al. 1986; Max and Korsmeyer 1985; Takahashi et al. 2000). J-chain cDNA sequencing revealed that mammalian J chains share well-conserved features among mouse, human, cow and brushtail possum (Adamski and Demmer 1999; Kulseth and Rogne 1994; Matsuuchi et al. 1986; Max and Korsmeyer 1985). The amphibian and avian J chains also have a high degree of homology to the cDNA sequences of mammals (Hohman et al. 1997; Takahashi et al. 2000). Although IgM and IgY have been found in reptiles (Kobayashi et al. 1973; Muthukkaruppan et al. 1982; Vaerman et al. 1975; Warr et al. 1995), the presence of J chain has not been documented thus far. Here, we have conducted experiments on the cloning and sequencing of the turtle (*Trachemys scripta*) J-chain cDNA using reverse transcriptase-polymerase chain reaction (RT-PCR) and rapid amplification of cDNA ends (RACE). In addition, J-chain mRNA and protein expression was examined by Northern blotting and immunohistochemistry, respectively. These results demonstrate that turtle J chain has highly conserved structural features similar to those of mammals, birds and amphibians, and suggest the presence of a mucosal immune system mediated by pIgs in reptiles.

Materials and methods

Turtles

Ten turtles (*Trachemys scripta)* were obtained from a dealer (Shimizu kingyo, Tokyo, Japan).

S2	(sense)	5'-GTTCTTGTTGACAACAAATG-3'
S4	(antisense)	5'-AGGATCACATTTTTTACAGA-3'
T-GSP-1	(sense)	5'-CGAAAGACAATCCCCAGGAAGAAGT-3'
3 sites adaptor primer	(antisense)	5'-CTGATCTAGAGGTACCGGATCC-3'
TS1	(sense)	5'-AGTTCCGATACCTGCTACACCTA-3'
TA1	(antisense)	5'-AGACAGCCGGTAGACAAAGGTGGTT-3'
TS2	(sense)	5'-TGACAGGAACAAATGCTACACCAC-3'
TA2	(antisense)	5'-CTCGTATGTTTCTCACCAGGACTTC-3'
RT primer (5'-phosphorylation)		5'-TTTTGGTCTGTGGGG-3'
T-J-C2	(sense)	5'-AGGCAGATGACACTCCTCTAAACTC-3'
T-J-C3	(antisense)	5'-GGGCAGATGACAGTATAACAAGGC-3'
T-J-C4	(sense)	5'-GGAATTCATGAAGACCTCTTTGTTACTGTGGG-3'
T-J-C6	(antisense)	5'-GGTCGACTTCTAATCAGCGTAGCAGGATTCTGGA-3'
Aac-1	(sense)	5'-TCGAACAAGAGATGGCAACTG-3'
Aac-2	(antisense)	5'-TTACGTTCAGGAGGAGCAATG-3'

Fig. 1 Primers used are S2 and S4 for RT-PCR; T-GSP-1 and 3 sites adaptor primer for 3′RACE; TS1, TA1, TS2, TA2 and RT primer (5′ phosphorylation) for 5′RACE; T-J-C2 and T-J-C3 for Northern and genomic Southern blotting; T-J-C4 and T-J-C6 for preparation of fusion protein; and Aac-1 and Aac-2 for β-actin

Preparation of RNA

Total RNA was extracted by ultracentrifugation methods (Zarlenga and Gamble 1987). Various tissues (stomach, intestine, spleen, lung and heart) from the turtle were dissected into small pieces and each homogenized in a solution containing 4 M guanidine thiocyanate, 25 mM sodium citrate (pH 7.0), 0.5% sarcosyl, and 0.1 M 2-mercaptoethanol. Samples were then layered onto cesium trifluoroacetate (Amersham Pharmacia Biotech, Little Chalfont, Buckinghamshire, UK) and centrifuged at 160,000 *g* for 16 h at 15 °C. After centrifugation, pellets were extensively washed with 70% ethanol and used as total RNA.

Cloning of turtle J-chain cDNA by RT-PCR

A random primed first-strand cDNA was synthesized from 1 μg of total RNA from turtle intestine, using 10 units of Rous-associated virus 2 reverse transcriptase (Takara shuzou, Kyoto, Japan) at 42 °C for 1 h. Turtle J-chain primers were used in PCR. cDNA was amplified in a buffer containing 2.5 mM dNTP, 20 pM of both primers and 1 unit of *Taq* DNA polymerase (Takara shuzou). PCR conditions (35 cycles) were as follows: denature for 1 min at 94 °C, annealing for 2 min at 50 °C and extension for 3 min at 72 °C. PCR products were electrophoresed through 1.8% agarose gels and a fragment that was hybridized with human J-chain cDNA by PCR Southern blotting (data not shown) was subcloned into the pT7 blue T vector (Novagen, Darmstadt, Germany) and then sequenced by Mega BACE 1000 (Molecular Dynamics, Sunnyvale, Calif., USA) using a DYEnamic ET dye terminator cycle sequence kit (Amersham Pharmacia Biotech). DNA sequences obtained were analyzed with Genetyx-Mac version 10.1.1 (Software Development, Tokyo, Japan).

In this study, seven kinds of primers were designed to obtain the PCR product of turtle J chain. These were designed through careful examination of sequence conservation patterns based on the published J-chain cDNA sequences of human, mouse, cow, *Xenopus laevis* and brushtail possum. Various combinations of primer sets were used for PCR and only a combination of S2 and S4 primers successfully functioned to obtain a J-chain product compatible with an expected size. The nucleotide sequences of the S2 and S4 primers are shown in Fig. 1.

3′RACE and 5′RACE

To obtain a full-length turtle J-chain cDNA, 3′RACE and 5′RACE were performed using a 3′- and 5′-full RACE core set (Takara shuzou) according to the manufacturer's instructions. Briefly, the cDNA was synthesized using 1 μg of total RNA, oligo dT-3 sites adaptor primer and reverse transcriptase for 3′RACE. PCR for 3′RACE was performed with J-chain-specific primer (T-GSP-1)

and three sites adaptor primer (Fig. 1). PCR conditions (35 cycles) were as follows: denature for 30 s at 94 °C, annealing for 30 s at 55 °C, and extension for 2 min at 72 °C. The PCR product was subcloned into the pT7 blue T vector (Novagen), then sequenced. Furthermore, cDNA was generated with 1 μg of total RNA and RT primer (Fig. 1) for 5′RACE. Intact 5′-end cDNA was obtained with nested PCR using TS1, TA1, TS2 and TA2 primers (Fig. 1), which were designed based on a partial sequence obtained by 3′RACE. The PCR product was subcloned into the pT7 blue T vector (Novagen) and then sequenced.

Northern blot analysis

Twenty micrograms of total RNA from stomach, intestine, spleen, lung or heart were electrophoresed through 1.5% agarose gels containing 6% formaldehyde and then transferred to nylon membranes. A partial J-chain cDNA fragment (578 bp) was synthesized by PCR using primers T-J-C2 and T-J-C3 (Fig. 1) as a probe. Hybridization was carried out with ^{32}P-labeled probe for 16 h at 42 °C in a solution containing 50% formamide, 0.65 M NaCl, 5×Denhardt's solution, 5 mM EDTA, 0.1% sodium dodecyl sulfate (SDS), 0.1 M Pipes-NaOH (pH 6.8), and 100 μg/ml salmon sperm DNA. The membrane was washed once with 2×SSC/0.1% SDS, and twice with 0.1×SSC/0.1% SDS at 60 °C for 30 min each, and then exposed to X-ray film for 17 h (Kodak, Rochester, N.Y.). As a control, the turtle β-actin probe was synthesized by RT-PCR, using Aac-1 and Aac-2 primers (Fig. 1). Their designs were based on conserved regions of nucleotide sequences among human (Ng et al. 1985), mouse (Tokunaga et al. 1986) and *Halocynthia roretzi* (Kusakabe et al. 1991) (data not shown).

Genomic Southern blotting

Ten micrograms of genomic DNA from turtle liver was digested with *Bam*HI, *Eco*RI, or *Xba*I for 12 h at 37 °C, and then electrophoresed through 0.7% agarose gels. Gels were treated with an alkaline solution (1.5 M NaCl, 0.2 M NaOH) for 60 min and denatured genomic DNA was transferred to a nylon membrane. The membrane was hybridized with a ^{32}P-labeled probe for 16 h at 65 °C in a solution containing 5×Denhardt's solution, 5×SSC, 0.1% SDS and 1 mg/ml salmon sperm DNA. After washing three times with 0.1×SSC and 0.1% SDS for 60 min at 65 °C, the membrane was exposed to X-ray film (Kodak) for 20 h. The same probe used for Northern blotting was utilized for the genomic Southern blotting.

Preparation of the turtle J-chain fusion protein

An open reading frame was amplified from full-length turtle J-chain cDNA by PCR using primers T-J-C4 and T-J-C6 (Fig. 1), which were designed with *Eco*RI or *Sal*I sites at the 5′ end, respectively. The PCR product was ligated into *Eco*RI and *Sal*I sites of the pET32a(+) vector (Novagen) and used to transform E. *coli* strain BL21 (DE3) (Novagen). Protein expression was induced by addition of 1 mM isopropyl-β-d-thiogalactopyranoside (IPTG) for 4 h at 37 °C. Cells were collected by centrifugation at 7,000 *g* and suspended in a buffer containing 5 mM imidazole, 0.5 M NaCl, 20 mM Tris-HCl (pH 7.9) and 6 M urea, then sonicated three times at intervals of 30 s on ice. Supernatant was collected by centrifugation at 15,000 *g* at 4 °C for 30 min, and then applied to His-Bind metal chelation resin (Novagen) according to the manufacturer's instructions. Purified fusion protein was dialyzed against phosphate buffered saline (PBS) containing 5 M urea and adjusted to a final protein concentration of 1 mg/ml, then assayed by SDS-PAGE.

Three rabbits were immunized intradermally with 0.2 mg of fusion protein emulsified in an equal volume of complete Freund's adjuvant, and then were boosted five times with an emulsion of fusion protein and incomplete Freund's adjuvant at two-week intervals. Two weeks after the last booster, the whole immune serum was isolated and applied to protein A column (Amersham Pharmacia Biotech) and then a polyclonal antibody to the turtle J-chain fusion protein was obtained. After titration, it was used for immunohistochemical staining as an anti-tortoise J-chain IgG. Furthermore, this antibody was absorbed with an excess amount of J-chain fusion protein (absorbed antibody) and used as a control.

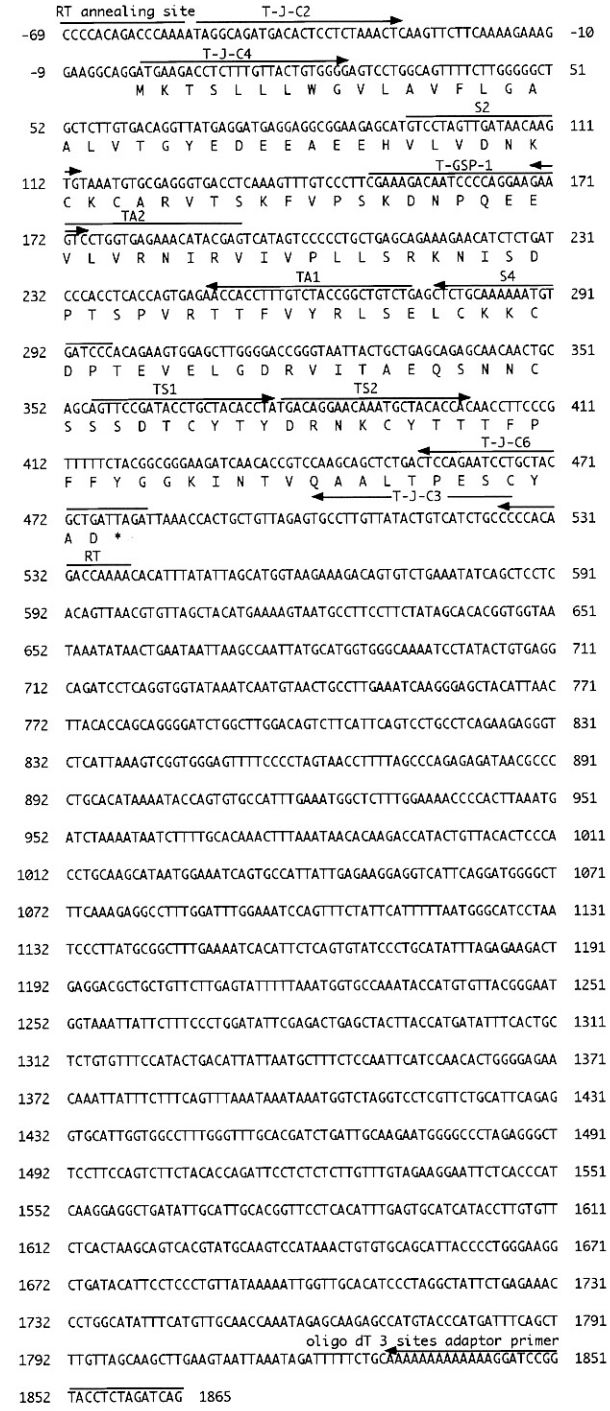

Fig. 2 Nucleotide sequences of turtle J-chain cDNA. *Arrows* and *solid line* indicating each primer site and nucleotide sequence are shown in Fig. 1. The nucleotide sequence data will appear in the DDBJ/EMBL/GenBank nucleotide sequence databases under accession number AB085611

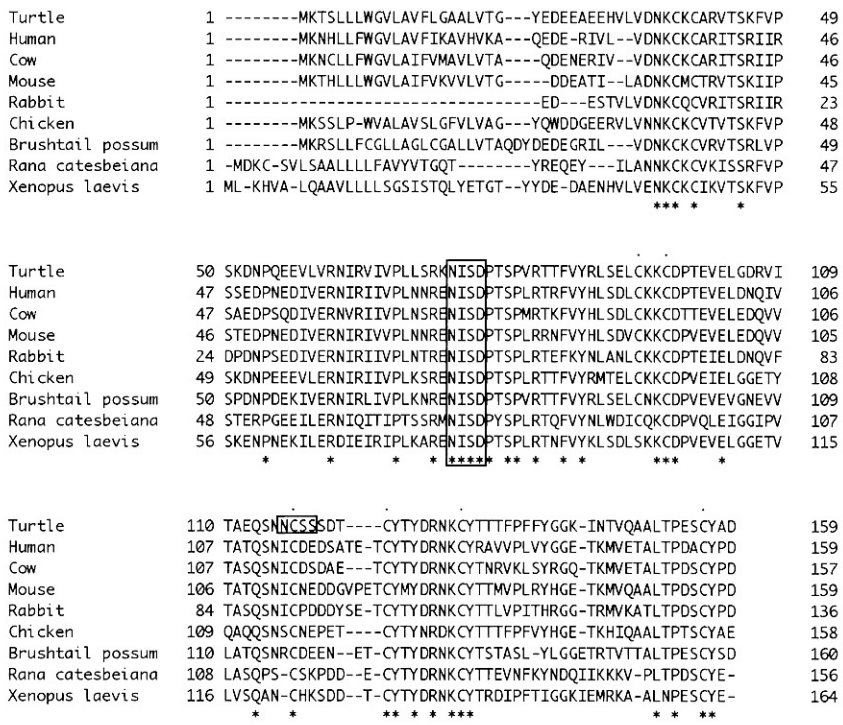

Fig. 3 Alignment of the amino acid sequences of J chains from human (Max and Korsmeyer 1985), cow (Kulseth and Rogne 1994), mouse (Matsuuchi et al. 1986), rabbit (Hughes et al. 1990), chicken (Takahashi et al. 2000), brushtail possum (Adamski and Demmer 1999), *Rana catesbeiana* (Mikoryak et al. 1988) and *Xenopus laevis* (Hohman et al. 1997). *Asterisks* indicate identical amino acid residues. *Dots* indicate cysteine residues. The Asn-linked glycosylation sites at position 74 and 116 are *boxed*. *Numbering* is according to the turtle J-chain sequence

Immunohistochemical method

Tissues from turtle intestine, spleen, stomach and liver were fixed in 96% ethanol at 4 °C for 16 h and then paraffin sections were subjected to immunoperoxidase staining. Briefly, endogenous peroxidase activity was blocked with 0.3% H_2O_2 in methanol for 30 min. After washing with PBS, sections were incubated with 10% normal goat serum to block non-specific reactions, and subsequently incubated with the anti-turtle J-chain antibody or absorbed antibody for 1 h at room temperature. After washing, sections were incubated with horseradish peroxidase-conjugated $F(ab')_2$ fragments of goat anti-rabbit immunoglobulins (Biosource International, Camarillo, Calif.) for 1 h at room temperature. The substrate reaction was performed in a solution containing 0.05% 3,3′-diaminobenzidine tetrahydrochloride and 0.005% H_2O_2 for 10 min at room temperature.

Results

The turtle J-chain PCR product, which at 204 bp has a relatively high homology to mammalian, avian and amphibian J chains, was obtained from total RNA by RT-PCR using S2 and S4 primers. To identify full-length turtle J-chain cDNA, sense primers were designed from the sequence of 204 bp for RACE. Both 3′RACE and 5′RACE were performed and 1717 bp and 827 bp products, respectively, were obtained and sequenced. After confirmation of the presence of a poly(A) site and ATG codon, a turtle J-chain cDNA sequence with 1,934 nucleotides was identified (Fig. 2). An open reading frame sequence was reconfirmed by RT-PCR using gene-specific T-J-C2 and T-J-C3 primers and used as a probe for Northern and genomic Southern blotting. As shown in Fig. 2, the open reading frame of turtle J chain consisted of 477 nucleotides, encoding 159 amino acid residues.

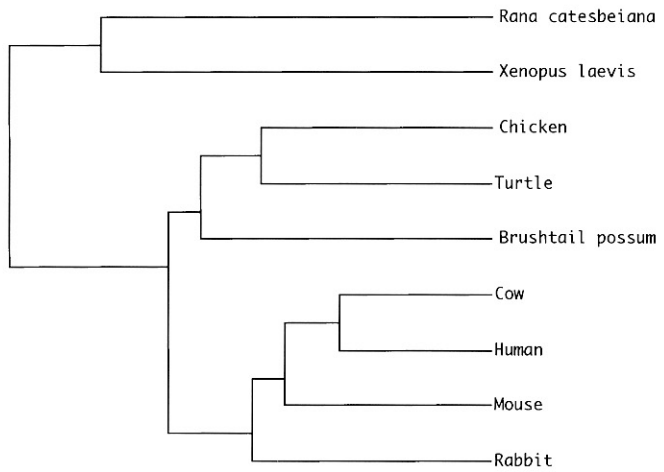

Fig. 4 Phylogenetic analysis of J chain from turtle, human, cow, mouse, rabbit, chicken, brushtail possum, *Rana catesbeiana* and *Xenopus laevis*. The phylogenetic tree was constructed using the Genetyx-Mac version 10.1.1 (Software Development) of the UPGMA method based on the nucleotide and deduced amino acid sequences

The turtle J-chain cDNA showed a high degree of homology to human (69%), mouse (67%), cow (69%), chicken (76%), brushtail possum (70%), *Rana catesbeiana* (57%) and *Xenopus laevis* (65%) J chains. The deduced amino acid sequences of the turtle J chain also showed a high degree of homology to human (60%), mouse (61%), cow (60%), rabbit (60%), chicken (69%), brushtail possum (65%), *R. catesbeiana* (47%) and *X. laevis* (58%). In addition, the positions of eight cysteine residues were conserved in these different species

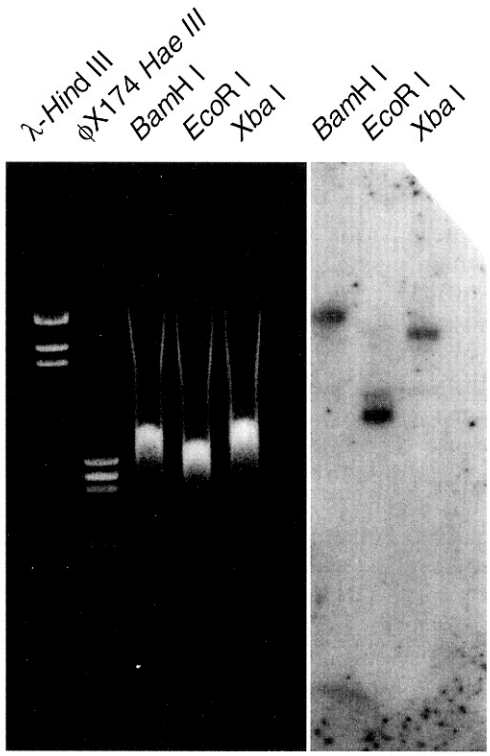

Fig. 5 Southern blot hybridization of turtle genomic DNA with the turtle J-chain probe. DNA (10 μg) was digested with *Bam*HI (23 kb), *Eco*RI (2.3 and 3.2 kb), or *Xba*I (16 kb), and electrophoresed through 0.7% agarose gels. The membrane was hybridized with the T-J-C2/3 PCR product probe, washed and exposed to X-ray film for 20 h

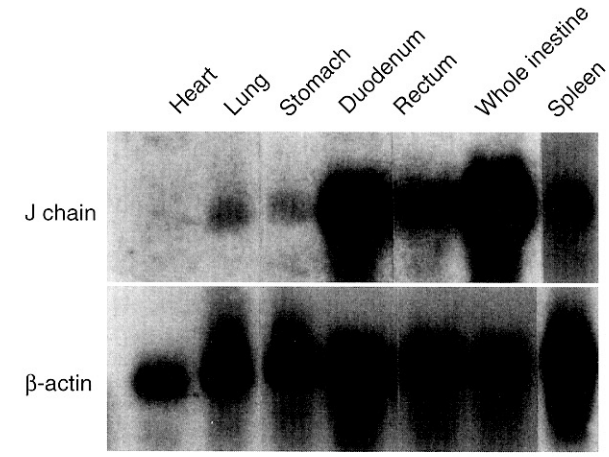

Fig. 6 Northern blot hybridization of turtle J-chain gene expression. Total RNA (20 μg) from various tissues was electrophoresed through 1.5% agarose/6% formaldehyde gels. The membrane was hybridized with the T-J-C2/3 PCR product probe, washed and exposed to X-ray film for 17 h

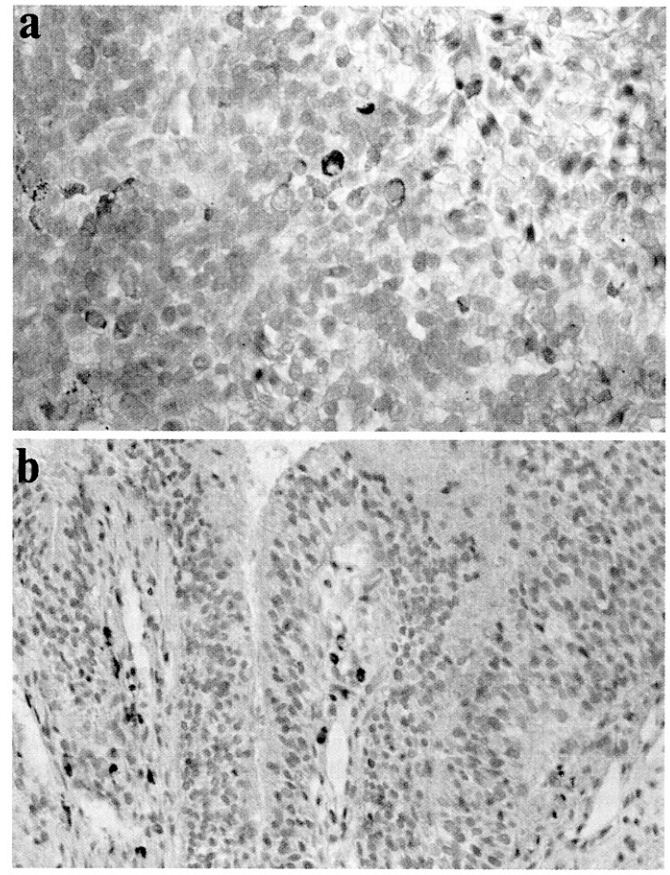

Fig. 7a, b Immunohistochemical analysis of J-chain protein in turtle. **a** Spleen; **b** Small intestine

(turtle, human, mouse, cow, rabbit, chicken, brushtail possum, *R. catesbeiana*) with only *X. laevis* being an exception (Fig. 3). Genetyx-Mac analysis revealed the presence of two N-glycosylation sites in the turtle J chain. One of these was found at an identical position as in the other eight animals (NISD), but the second (NCSS) has not been described before.

Phylogenetic tree analysis performed by the Genetyx-Mac version 10.1.1 of the UPGMA method based on nucleotide and deduced amino acid sequences indicated that turtle J chain is more closely related to chicken than to the other species examined (Fig. 4). Genomic Southern blotting analysis revealed a 23-kb and 16-kb single band following *Bam*HI or *Xba*I digestion, respectively. In contrast, *Eco*RI digestion resulted in the appearance of two bands of 2.3 kb and 3.2 kb (Fig. 5). To examine the expression of J-chain mRNA, RNA extracted from various turtle tissues was examined by Northern blotting. J-chain mRNA was detected in lung, stomach, duodenum, rectum and spleen (Fig. 6). A high level of expression was observed in the small intestine. However, no J-chain expression was observed in heart.

Because no anti-turtle J-chain antibody suitable for use in immunohistochemistry was commercially available, we developed an antibody to turtle J-chain fusion protein using the pET32a(+) vector system. Induction by IPTG resulted in the formation of a fusion protein of M_r ~40,000 (data not shown). This fusion protein, emulsified in adjuvant, was injected into rabbits, and anti-turtle J-chain sera were obtained. Immunohistochemical staining revealed the presence of J-chain protein in plas-

ma cells of splenic white pulp. A relatively large number of J-chain-positive plasma cells were localized around the white pulp, but only a small number actually in the white pulp. A small number of positive cells were also present in the red pulp. A large number of J-chain-positive plasma cells was detected in the submucosa of the small intestine (Fig. 7a, b). No J-chain-positive cells were detected in spleen and small intestine when absorbed antibody was used as the first antibody instead of an anti-turtle J-chain IgG.

Discussion

The turtle J-chain cDNA, as determined in this study, consists of a total of 1,934 bp, containing the signal peptides, a 1,350-bp 3′ untranslated region, and an open reading frame composed of 477 bp, encoding 159 amino acid residues. According to the criteria given by von Heijne (1985), the deduced cleavage site of the signal peptide is glycine or valine at position –1 or –3, respectively. Therefore, mature turtle J chain is composed of 137 amino acids, M_r ~15,000, making it identical to other animal species such as human (Max and Korsmeyer 1985), mouse (Matsuuchi et al. 1986), cow (Kulseth and Rogne 1994) and chicken (Takahashi et al 2000).

Based on the deduced amino acid sequence, the positions of the eight cysteine residues in turtle were identical to those established in other species, with the exception of *Xenopus laevis* (Fig. 3). This suggests that the positions of the cysteine residues in the J chain are well conserved through evolution from reptiles to mammals. A phylogenetic tree based on J-chain amino acid sequences indicated two different but closely linked clusters with common ancestors, one being amphibians and the other the remaining species, including mammals, birds and reptiles. Furthermore, the turtle J chain is more closely related to chicken than to *Rana catesbeiana* and *X. laevis*, suggesting that no significant gene mutations accumulated during the evolutionary process from reptile to bird. On the other hand, database analysis revealed two N-glycosylation sites in the turtle J chain. One is at a position identical in all eight animals, but the other has not been previously reported, suggesting a different composition of oligosaccharide chains in turtle. Although the function of the additional N-glycosylation site is not clarified, we hypothesize that it plays some important role in the formation, transport and secretion of turtle pIgs.

Mouse pentameric, but not hexameric, IgM contains the J chain (Koshland 1989). It has been reported that IgM does exist in reptiles, but whether the J chain was present was previously unclear (Kobayashi et al. 1973; Muthukkaruppan et al. 1982; Vaerman et al. 1975). Here, we have investigated the presence of J chain in turtle. It becomes clear that J-chain mRNA and protein are present in turtle, but the association of J chain in turtle IgM or IgY is still unclear. Previously, partial cDNA sequences of turtle IgM have been reported (Turchin and Hsu 1996). By comparison of Cμ3 and Cμ4 between human and turtle, five cysteine residues were shown to be well conserved. The human J chain binds to pentameric IgM via disulfide bonds involving the penultimate cysteine residue in the secretory tailpiece of the μ heavy chain (Mestecky et al. 1999). Because five cysteine residues in turtle IgM were located at the same position as in human, it is speculated that turtle J chain may also bind to the penultimate cysteine residue of IgM.

Because the genomic structure of the turtle J-chain gene has not been previously described, genomic Southern blotting was performed to determine the number of J-chain genes in this species. From this, we concluded that because digestion of genomic DNA by *Bam*HI or *Xba*I each resulted in the appearance of a single band the turtle J-chain gene is a single copy gene, as reported for the amphibian J chain. However, genomic Southern blotting also revealed two bands, approximately 3 kb and 2.3 kb, in turtle DNA digested with *Eco*RI, demonstrating that the turtle J chain gene has an *Eco*RI site in the intron, because no *Eco*RI site was detected in the nucleotide sequence used as a probe. On the other hand, other studies have reported two types of human J-chain genes, a functional gene and pseudogene, which were identified by genomic Southern blotting using DNA digested with *Eco*RI. This suggests the possibility that there is a similar turtle J-chain pseudogene, as found in human and monkey (Max et al. 1986, 1994). Further study is required to determine the exon/intron organization of the turtle J-chain gene.

The J chain is closely associated with SIgA and SIgM, which play an important role in the mucosal immune system (Mestecky and McGhee 1987). It has been reported that tortoise bile and intestinal secretions largely contain 19S Ig (considered to be IgM) and that many cells in the lamina propria of tortoise intestine were stained with an anti-19S antibody (Vaerman et al. 1975). In the present study, expression of J-chain mRNA was observed in lung, stomach, duodenum and rectum, suggesting that J chain in turtle may contribute to the mucosal immune system, as it does in mammals. The spleen is considered to be a lymphopoietic organ in reptiles (Muthukkaruppan et al. 1982) and J-chain mRNA expression was also detected in this organ in the turtle. An immunohistological study revealed that J-chain protein was present in spleen and intestine. Taken together, our results suggest that there may be a mucosal immune system in turtle, and J chain may contribute to the defense of mucosal sites in this species.

Acknowledgements We thank Dr. Susumu Tomonaga for helpful discussions and comments on the manuscript. This work was supported in part by grants from the General Joint Research Grant for Nihon University, and from The Promotion and Mutual Aid Corporation for Private Schools of Japan.

References

Adamski FM, Demmer J (1999) Two stages of increased IgA transfer during lactation in the marsupial, *Trichosurus vulpecula* (Burushtail possum). J Immunol 162:6009–6015

Brandtzaeg P (1974) Presence of J chain in human immunocytes containing various immunoglobulin classes. Nature 252:418–420

Brandtzaeg P (1985) Role of J chain and secretory component in receptor-mediated glandular and hepatic transport of immunoglobulins in man. Scand J Immunol 22:111–145

Brewer JW, Randall TD, Parkhause REM, Coley RB (1994) IgM hexamers? Immunol Today 15:165–168

Cattaneo A, Neuberger MS (1987) Polymeric immunoglobulin M is secreted by transfectants of non-lymphoid cells in the absence of immunoglobulin J chain. EMBO J 6:2753–2758

Davis AC, Roux KH, Pursey J, Shulman MJ (1989) Intermolecular disulfide bonding in IgM: effects of replacing cysteine residues in the μ heavy chain. EMBO J 8:2519–2526

Hohman VS, Stewart SE, Willett CE, Steiner LA (1997) Sequence and expression pattern of J chain in the amphibian, *Xenopus laevis*. Mol Immunol 34:995–1002

Hughes GJ, Frutiger S, Paquet N, Jaton JC (1990) The amino acid sequence of rabbit J chain in secretory immunoglobulin A. Biochem J 271:641–647

Iwase T, Saito I, Takahashi T, Chu L, Usami T, Mestecky J, Moro I (1993) Early expression of human J chain and μ chain gene in the fetal liver. Cell Struct Funct 18:297–302

Johansen FE, Braathen R, Brandtzaeg P (2000) Role of J chain in secretory immunoglobulin formation. Scand J Immunol 52:240–248

Kaji H, Parkhouse RME (1974) Intracellular J chain in mouse plasmacytomas secreting IgA, IgM and IgG. Nature 249:45–47

Kimura M, Takahashi T, Iwata A, Matsumoto N, Ogura Y, Akagi T, Akima S, Kobayashi K, Moro I (2001) Ontogeny of the murine Ig joining chain gene and protein. Scand J Immunol 54:613–618

Kobayashi K, Vaerman JP, Bazin H, LeBacq-Verheyden AM, Heremans JF (1973) Identification of J-chain in polymeric immunoglobulins from a variety of species by cross-reaction with rabbit antisera to human J-chain. J Immunol 111:1590–1594

Koshland ME (1985) The coming of age of the immunoglobulin J chain. Annu Rev Immunol 3:425–457

Koshland ME (1989) The immunoglobulin helper: the J chain. In: Honjo T, Alt FW, Rabbitts TH (eds) Immunoglobulin gene XVII. Academic Press, London, pp 345–359

Kulseth MA, Rogne S (1994) Cloning and characterization of the bovine immunoglobulin J chain cDNA and its promoter region. DNA Cell Biol 13:37–42

Kusakabe T, Suzuki J, Saiga H, Jeffery WR, Makabe KW, Satoh N (1991) Temporal and spatial expression of a muscle actin gene during embryogenesis of the ascidian *Halocynthia roretzi*. Dev Growth Differ 33:227–234

Matsuuchi L, Cann GM, Koshland ME (1986) Immunoglobulin J chain gene from the mouse. Proc Natl Acad Sci USA 83:456–460

Max EE, Korsmeyer SJ (1985) Human J chain gene: structure and expression in B lymphoid cells. J Exp Med 161:832–849

Max EE, McBride OW, Morton CC, Robinson MA (1986) Human J chain gene: chromosomal localization and associated restriction fragment length polymorphisms. Proc Natl Acad Sci USA 83:5592–5596

Max EE, Jahan N, Yi H, McBride WO (1994) A processed J chain pseudogene on human chromosome 8 that is shared by several primate species. Mol Immunol 131:1029–1036

Mestecky J, McGhee JR (1987) Immunoglobulin A (IgA): molecular and cellular interactions involved in IgA biosynthesis and immune response. Adv Immunol 40:153–245

Mestecky J, Winchester RJ, Hoffman T, Kunkel HG (1977) Parallel synthesis of immunoglobulin and J chain in pokeweed mitogen-stimulated normal cells and in lymphoblastoid cell lines. J Exp Med 145:760–765

Mestecky J, Moro I, Moldoveanu Z, Takahashi T, Iwase T, Kubagawa H, Cooper MD (1997) Immunoglobulin J chain: an early differentiation marker of human B cells. Ann NY Acad Sci 815:111–113

Mestecky J, Moro I, Underdown BI (1999) Mucosal immunoglobulins. In: Ogra PL, Mestecky J, Lamm ME, Strober W, Bienenstock J, McGhee JR (eds) Mucosal immunology, 2nd edn. Academic Press, New York, pp 133–152

Mikoryak CA, Margolies MN, Steiner LA (1988) J chain in *Rana catesbeiana* high molecular weight Ig. J Immunol 140:4279–4285

Muthukkaruppan VR, Borysenko M, Ridi RE (1982) RES structure and function of the reptilia. In: Cohen N, Sigel MM (eds) The reticuloendothelial system. A comprehensive treatise, vol 3. Phylogeny and ontogeny. Plenum Press, New York, pp 461–508

Ng SY, Gunning P, Eddy R, Ponte P, Leavitt J, Shows T, Kedes L (1985) Evolution of the functional human β actin gene and its multi-pseudogene family: conservation of noncoding regions and chromosomal dispersion of pseudogenes. Mol Cell Biol 5:2720–2732

Randall TD, King LB, Corley RB (1990) The biological effects of IgM hexamer formation. Eur J Immunol 20:1971–1979

Randall TD, Brewer JW, Corley RB (1992) Direct evidence that J chain regulates the polymeric structure of IgM in antibody-secreting B cells. J Biol Chem 267:18002–18007

Takahashi T, Iwase T, Tachibana T, Komiyama K, Kobayashi K, Chen CH, Mestecky J, Moro I (2000) Cloning and expression of the chicken immunoglobulin joining (J)-chain cDNA. Immunogenetics 51:85–91

Takahashi T, Kimura M, Matsumoto N, Iwata A, Ogura Y, Yoshida T, Kamei N, Komiyama K, Mestecky J, Moro I (2002) Cloning of the chicken immunoglobulin joining (J)-chain gene and characterization of its promoter region. DNA Cell Biol 21:81–90

Tokunaga K, Taniguchi H, Yoda K, Shimizu M, Sakiyama S (1986) Nucleotide sequence of a full-length cDNA for mouse cytoskeletal β actin mRNA. Nucleic Acids Res 14:2829

Turchin A, Hsu E (1996) The generation of antibody diversity in the turtle. J Immunol 156:3797–3805

Vaerman JP, Picard J, Heremans JF (1975) Structural data on chicken IgA and failure to identify the IgA of the tortoise. Adv Exp Med Biol 64:185–195

Von Heijne G (1985) Signal sequences. The limits of variation. J Mol Biol 184: 99–105

Warr GW, Magor KE, Higgins DA (1995) IgY: clues to the origins of modern antibodies. Immunol Today 16: 392–398

Zarlenga DS, Gamble HR (1987) Simultaneous isolation of preparative amounts of RNA and DNA from *Trichinella spiralis* by cesium trifluoroacetate isopycnic centrifugation. Anal Biochem 162:569–574

Clin Exp Immunol 2004; **137**:52–58 doi:10.1111/j.1365-2249.2004.02487.x

Dietary fructooligosaccharides up-regulate immunoglobulin A response and polymeric immunoglobulin receptor expression in intestines of infant mice

Y. NAKAMURA, S. NOSAKA, M. SUZUKI, S. NAGAFUCHI, T. TAKAHASHI, T. YAJIMA, N. TAKENOUCHI-OHKUBO*, T. IWASE* & I. MORO* *Department of Nutritional Research, Nutrition Science Institute, Meiji Dairies Corporation, Kanagawa, Japan, and *Department of Pathology, Nihon University School of Dentistry, Tokyo, Japan*

(Accepted for publication 25 March 2004)

SUMMARY

We examined whether or not dietary fructooligosaccharides (FOS) in infancy can have a beneficial effect on the mucosal immune system. Newborn BALB/c mice, accompanied by their dams until 21 days of age, were fed either a control diet based on casein [FOS(–) diet group] or a FOS(–) diet supplemented with 5% (w/w) FOS [FOS(+) diet group]. Total IgA levels in tissue extracts from the intestines of mice in the FOS(+) diet group at 38 days of age were about twofold higher ($P < 0{\cdot}05$) than those in the FOS(–) diet group in the jejunum, ileum and colon. Ileal and colonic polymeric immunoglobulin receptor (pIgR) expression in the FOS(+) diet group at 36 days of age was 1·5-fold higher than in the FOS(–) diet group ($P < 0{\cdot}05$). Consistent with these results, the ileal IgA secretion rate of the FOS(+) diet group at 37 days of age was twofold higher than that of the FOS(–) diet group ($P < 0{\cdot}05$). Moreover, the percentage of $B220^{+}IgA^{+}$ cells in Peyer's patches (PP) was significantly higher in the FOS(+) diet group than in the FOS(–) diet group (6·2% *versus* 4·3%, $P < 0{\cdot}05$), suggesting that isotype switching from IgM to IgA in PP B cells might be enhanced *in vivo*. Taken together, our findings suggest that dietary FOS increases the intestinal IgA response and pIgR expression in the small intestine as well as the colon in infant mice.

Keywords fructooligosaccharides immunoglobulin A polymeric immunoglobulin receptor prebiotics

INTRODUCTION

Fructooligosaccharides (FOS) exist in a number of edible plants, such as onion and edible burdock, and are produced commercially by the action of fructosyltransferase on sucrose [1]. FOS are representative prebiotics: food products that escape digestion by pancreatic and small-intestinal enzymes in the human gut and therefore reach the colon, where they have beneficial effects. It has been reported that dietary FOS influences many aspects of intestinal function through fermentation [2].

Yamamoto *et al.* [3] and Juffrie [4] have reported that dietary FOS improve the faecal content and reduce the frequency of diarrhoea in infants, respectively. Numerous studies in adults or aged humans have shown that dietary FOS lead to an increase in faecal bifidobacteria numbers [1,5–7]. Because bifidobacteria, which are probiotics, are presumed to be antagonistic to pathogenic bacteria and to promote non-specific stimulation of the immune system, it is possible that the mechanisms by which dietary FOS confer beneficial effects on the host may include immunomodulatory effects on the intestinal immune system through the increase in bifidobacteria numbers.

There have been a few reports on the effect of dietary FOS on the mucosal immune system. Pierre *et al.* [8] demonstrated that dietary FOS enhanced the development of the gut-associated lymphoid tissue, and Hosono *et al.* [9] showed that dietary FOS up-regulated the faecal IgA content in the adult mouse. Furthermore, Swanson *et al.* [10] indicated that FOS plus mannanoligosaccharides influenced ileal IgA in the adult dog.

As the intestinal immune system in infants is immature compared to that in adults, it is of interest to investigate the effect of prebiotics on the intestinal immune system in infancy. Therefore, we have studied the effects of FOS ingestion on the mucosal IgA response and pIgR expression in the intestines of infant mice.

MATERIALS AND METHODS

Animals

Timed-pregnant BALB/c mice were purchased from Japan SLC (Shizuoka, Japan) and were maintained in individual plastic

Correspondence: Y. Nakamura, Department of Nutritional Research, Nutrition Science Institute, Meiji Dairies Corporation, Kanagawa 250–0862, Japan.

E-mail: YOSHITAKA_1_NAKAMURA@MEIJI-MILK.COM

cages. The mice ate a non-purified diet (MF; Oriental Yeast, Tokyo, Japan) and drank water, both *ad libitum*. The day of birth is referred to as day 0. At 2 days of age, the litter sizes were adjusted to four to six pups on the basis of comparable mean body weight. Each dam and her pups were placed together in their own plastic cage. The dams were fed a control diet *ad libitum* based on casein [the FOS(–) diet] or on the FOS(–) diet supplemented with 5% (w/w) FOS [the FOS(+) diet] (Table 1). The added FOS (Meioligo-P®) were obtained from Meiji Seika Kaisya, Ltd (Tokyo, Japan). Pups were weaned at 21 days of age, and fed the same diets *ad libitum* until analysis. All procedures were approved by our institute's Committee for Research on Experimental Animals, and were conducted in accordance with the NRC Guide for the Care and Use of Laboratory Animals (1985).

Preparation of intestinal tissue samples and plasma membranes of the intestine

The procedure for the preparation of tissue samples from the small intestine and colon was a modification of a protocol described previously by our group [11]. Pups were killed under anaesthesia and the small intestine and colon were removed carefully from FOS(–) or FOS(+) diet-fed pups at 23, 30, 38 and 44 days of age. The small intestine from the pylorus to the ileocaecal junction was divided into two equal segments, defined as the jejunum and ileum. The luminal contents were flushed out with ice-cold phosphate buffered saline (PBS). Each segment was weighed after being washed. Then a 20-fold volume of PBS containing 1 mmol/l phenylmethylsulphonyl fluoride, 5 mmol/l EDTA, 100 μg/ml soybean trypsin inhibitor, 100 μg/ml leupeptin and 100 KIU/ml aprotinin in 50 mmol/l Tris-HCl (pH 6·8) was added, and the tissue was homogenized on ice using a Polytron homogenizer (Kinematica AG, Littau, Switzerland; setting 6; 30 s, three times). The suspension was centrifuged at 10 000 ***g*** for 15 min, and the supernatant obtained equalled the tissue extract used for the detection of intestinal IgA levels.

Intestinal plasma membranes were prepared from the suspension as described previously [12]. Briefly, intestinal suspensions were centrifuged (750 ***g*** for 10 min) to remove cells and nuclei. Membranes were pelleted from the supernatant by centrifugation (100 000 ***g*** for 30 min), resuspended and boiled (5 min) in Laemmli sample buffer for sodium dodecyl sulphate-polyacrylamide gel electrophoresis (SDS-PAGE) [13].

Table 1. Composition of the FOS(–) diet (g/kg)

Ingredient	FOS(–) diet
Casein	220
Sucrose	50
Starch	600
Cellulose	30
Soybean oil	50
Vitamins[1]	10
Minerals[2]	40

[1]The composition was as follows (IU/kg): vitamin A, 2 000 000; 7-dehydrocholesterol, 200 000; α-tocopheryl acetate (in g/kg): 10; menadione, 1; *p*-aminobenzoic acid, 10; inositol, 10; niacin, 4; calcium pantothenate, 4; choline chloride, 230·6; riboflavin, 0·8; thiamine HCl, 0·5; pyridoxine HCl, 0·5; folic acid, 0·2; D-biotin, 0·04; cyanocobalamine, 0·003. [2]The composition was as follows (in g/kg): NaCl, 139·3; KI, 0·79; KH_2PO_4, 389; $MgCO_3$, 40·2; $CaCO_3$, 381·4; Fe fumarate, 16·5; $MnCO_3$, 3·05; $ZnCO_3$, 0·58; $CuSO_4$ $5H_2O$, 0·6; $CoCl_2$, 0·023.

Faecal sample preparation

Faecal samples were prepared as described by deVos and Dick, with modifications [14]. At 28, 36 and 42 days of age, pups were placed into stainless-steel wire-mesh cages without bedding materials for 24 h individually, and the faecal samples were collected. The material was lyophilized and dissolved in 50 volumes of PBS containing 0·5 mmol/l EDTA and 100 μg/ml soybean trypsin inhibitor. The sample was then homogenized on ice using a Polytron homogenizer (30 s, three times) and centrifuged at 1600 ***g*** for 15 min, and the supernatant equalled the extract used for the detection of faecal IgA levels.

Collection of ileal secretions

Ileal secretion was collected from isolated intestinal loops of anaesthetized mouse pups using a modified version of that described by Ahnen *et al.* [12]. At 37 days of age, pups ($n = 6$) were anaesthetized with sodium pentobarbital (100 mg/kg) injected intraperitoneally. Then, a 6–8-cm section of ileum beginning at the ileo–caecal junction was isolated. The loop was washed with PBS to remove luminal contents and ligated at both ends. After 30 min, the loops were excised and the luminal content was flushed out with PBS containing 10 mg/ml soybean trypsin inhibitor (5 ml × 3). The sample volume was increased to 20 ml by adding PBS, and then the sample was centrifuged at 750 ***g*** for 15 min. The supernatant was used for measuring the IgA concentration.

Cell culture

Peyer's patches (PP) from FOS(–) or FOS(+) diet-fed pups ($n = 6$) at 35 days of age were used for the cultures. A single-cell suspension of PP was prepared as described previously [15]. In brief, PP dissected from the small intestine were placed in 10 ml of RPMI-1640 medium (GIBCO, Grand Island, NY, USA) in a glass dish, and then dissociated mechanically. The treated cells were washed twice with the RPMI-1640 medium. The PP cells (5×10^5 cells/0·2 ml/well) were cultured in triplicate in flat-bottomed, 96-well microtest plates (Falcon, Becton Dickinson, Franklin Lakes, NJ, USA) in RPMI-1640 medium containing 100 U/ml of penicillin (GIBCO), 100 μg/ml of streptomycin (GIBCO), 5 10^{-5} mol/l 2-mercaptoethanol and 10% heat-inactivated fetal bovine serum. The cells were incubated for 7 days at 37°C under 5% CO_2 in air. The culture supernatants were collected and stored at −80°C until assayed.

Enzyme-linked immunosorbent assay (ELISA)

Total IgA concentration was measured by enzyme linked immunosorbent assay (ELISA). At 4°C overnight, 96-well microtitre plates (Nunc, Roskilde, Denmark) were coated with 100 μl of rat antimouse IgA antibodies (Pharmingen, San Diego, CA, USA) (1 μg/ml) dissolved in 0·15 M PBS. The unbound antibodies were removed by three washes with 125 μl of PBS containing 0·05% (w/v) Tween 20 (PBS-T). The plates were incubated with 125 μl of 1% (w/v) bovine serum albumin (BSA) (Intergen, Purchase, NY, USA) for 30 min at room temperature and washed with PBS-T three times. Intestinal tissue extracts, faecal samples, ileal secretions, culture supernatants or standard mouse IgA (mouse myeloma protein; ICN Biomedicals, Costa Mesa, CA, USA) were diluted with 0·01 mol/l PBS (pH 7·2) containing 0·5 mol/l NaCl

and 0·1% Tween 20. The diluted samples or standards were added to the wells in triplicate. For each sample, an uncoated well blocked with 1% BSA was used as a control for non-specific binding. After incubation overnight at 4°C the plates were washed, and 100 μl of biotinylated rat antimouse IgA antibodies (Pharmingen) (50 ng/ml) were added. Following further incubation at room temperature for 2 h, the plates were washed and 100 μl of alkaline phosphatase-conjugated avidin (Organon Teknika, Durham, NC, USA) (1 μg/ml) were added to each well. Finally, 100 μl of *p*-nitrophenyl phosphate (1 mg/ml) dissolved in a diethanolamine buffer (pH 9·8) were added. After incubation at room temperature for 30 min, colour development was stopped by adding 50 μl of 5 mol/l NaOH, and then the absorbance at 405 nm of each well was measured. The total IgA content of each sample was calculated by means of a standard curve.

SDS-PAGE and antipolymeric immunoglobulin receptor immunoblotting

Antimouse polymeric immunoglobulin receptor (pIgR) antiserum was prepared in our laboratory. The procedure for preparing pIgR proteins followed the method described by Symersky *et al.* [16] with slight modifications. The BamH I-Sac I fragment of mouse pIgR cDNA was ligated with the pET32c vector. The mouse pIgR cDNA was kindly provided by Dr C. S. Kaetzel, University of Kentucky. The resultant plasmid was used to transform the BL21(DE3) strain of *E. coli*. After transformation the *E. coli* were incubated with shaking at 37°C until the OD 600 reached 0·6, then the bacteria were incubated with fresh TB medium containing 1 mM isopropyl-thio-β-D-galactopyranoside (IPTG) for 2 h at 37°C. The PITG-induced cells were collected by centrifugation, and crude fusion proteins were extracted in binding buffer (20 mM Tris-HCl pH 8·0, 5 mM imidazole, 500 mM NaCl) by sonication. The fusion proteins were purified by His binding column chromatography. Rabbits were immunized with the purified fusion proteins in Freund's complete adjuvant every 2 weeks for 3 months. Rabbit antimouse pIgR antiserum was obtained at 5 days after the last immunization.

Intestinal pIgR was measured by immunoblotting. The intestinal plasma membranes were subjected to 7·5% SDS-PAGE under reducing conditions [13]. The separated proteins were transferred electrophoretically to a nitrocellulose membrane (Hybond C extra, Amersham International plc, Bucks, UK) and immunostained with the rabbit antimouse pIgR antiserum (×500) followed by horseradish peroxidase-conjugated goat antirabbit IgG antibodies (Zymed Laboratory, South San Francisco, CA, USA) (×10 000). Molecular weight markers (Bio-Rad Laboratories, Hercules, CA, USA) were used on each gel and the relative values of pIgR were estimated by densitometric scanning. The values were expressed relative to the average value in FOS(–) diet group that was normalized to 100.

Identification of PP cell phenotype by flow cytometry

PP cells from FOS(–) or FOS(+) diet-fed pups at 35 days of age ($n = 5$–6) were prepared as described above and used for two-colour FACS analysis. The antibodies used for flow cytometry were fluorescein isothiocyanate (FITC)-labelled antimouse IgA (C10-3; Pharmingen) (1 μg/ml), FITC-labelled antimouse IgM (1B4B1; eBioscience, San Diego, CA, USA) (1 μg/ml), and phycoerythrin (PE)-labelled antimouse B220 (RA3–6B2; Pharmingen) (40 ng/ml) antibodies. All incubations were performed in the dark. Cells were incubated for 30 min on ice with FITC-labelled and PE-labelled antibodies. The cells were then washed in PBS. Stained cells were analysed with an EPICS XL (Beckman Coulter Inc., Hialeah, FL, USA). The data were analysed with SYSTEM II software (Beckman Coulter Inc.).

Caecal short-chain fatty acids

Caecal short-chain fatty acids (SCFA; acetic, propionic and *n*-butyric acids) were measured using high performance liquid chromatography (HPLC) (Shimadu, Kyoto, Japan) by the internal standard method, as described previously [17]. Briefly, pups were sacrificed under anaesthesia and the caecum was removed carefully from FOS(–) or FOS(+) diet-fed pups at 36 days of age. Caecal contents were homogenized by ultrasonication (Sonifier 250, Branson, Danbury, CT, USA) with crotonic acid and then centrifuged (750 ***g***). Fat-soluble substances in the supernatant were removed by extraction with chloroform. SCFA were separated using an ion exclusion column and detected using a post-column pH-buffered electroconductivity detection method. Caecal SCFA concentrations were expressed as mmol/kg caecal water.

Statistical analysis

The experimental data were expressed as means with their standard deviations for three to six pups per group. Differences were evaluated by the Student's *t*-test, the Mann–Whitney *U*-test or two-way ANOVA with Tukey–Kramer's *post hoc* test using the StatView 4·0 program (Abacus Concept Inc., Berkeley, CA, USA). Differences were considered to be significant at $P < 0.05$.

RESULTS

Effect of dietary FOS on total IgA levels in intestinal tissue extracts

Throughout the experiments, the food intake and body weight did not differ between the FOS(–) and FOS(+) diet group (data not shown). The total IgA levels in the intestinal tissue extracts were higher ($P < 0.05$) in the FOS(+) compared with the FOS(–) diet group in the jejunum, ileum and colon (Table 2). In the jejunum, the IgA levels in the FOS(+) diet group were significantly higher at 30, 38 and 44 days of age than the respective levels in the FOS(–) diet group. This was especially noticeable at 38 days of age, when the IgA level of the FOS(+) diet group was about two-fold higher than that of the FOS(–) diet group. Almost identical results were obtained for the ileum (38 days of age) and the colon (30 and 38 days of age).

Effect of dietary FOS on ileal IgA secretion and intestinal pIgR expression

The IgA content of dry matter faeces from the FOS(+) diet group at 36 days of age was significantly higher than that of the FOS(–) diet group (Fig. 1). This seemed to be due to an increase of intestinal IgA levels. However, it is accepted that some quantities of secretory IgA in the faeces are transported originally from the circulation into the bile in mice [18]. To eliminate the bilious secretory IgA contamination, we further examined the effect of dietary FOS on ileal IgA secretion by means of the intestinal loop method. The rate of ileal IgA secretion at 37 days of age was significantly higher in the FOS(+) compared with the FOS(–) diet group (Fig. 2). Moreover, ileal and colonic, but not jejunal, pIgR expression were significantly higher in the FOS(+) compared with the FOS(–) diet group (Fig. 3).

Table 2. Effect of dietary FOS on the total IgA levels in intestinal tissue extracts[1]

Intestinal IgA (μg/g)	Age (days)	FOS(−) Mean	FOS(−) s.d.	FOS(−) *n*	FOS(+) Mean	FOS(+) s.d.	FOS(+) *n*
Jejunum	23	46	28	6	42	14	4
	30	96	29	6	167*	71	6
	38	145	33	6	347*	89	6
	44	307	48	6	384*	49	6
Ileum	23	9	5	6	10	5	4
	30	38	22	6	69	46	6
	38	121	35	6	228*	71	6
	44	252	38	6	281	36	6
Colon	23	17	10	6	19	11	4
	30	117	39	6	219*	67	6
	38	202	31	6	399*	47	6
	44	345	103	6	365	89	6

FOS: fructooligosaccharides; s.d.: standard deviation. [1]The FOS(+) diet includes 5% fructooligosaccharides (Meiji Seika Kaisya, Ltd, Tokyo, Japan) + 95% (−) diet (for details of the FOS(−) diet, see Table 1. *Significant difference from the FOS(−) diet group ($P < 0.05$) by two-way ANOVA with Tukey–Kramer's *post hoc* test.

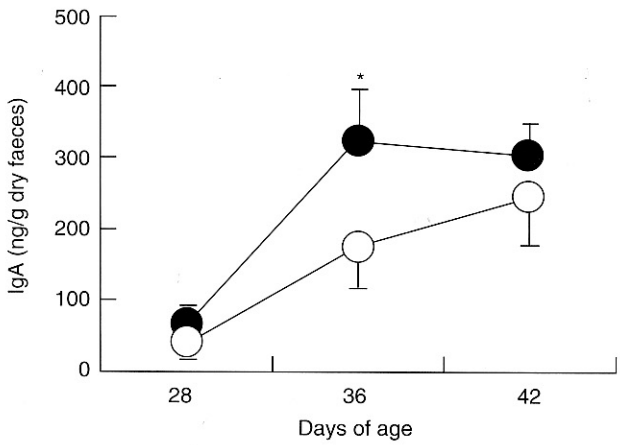

Fig. 1. Effect of dietary FOS on faecal IgA levels in mouse pups. The faecal IgA levels were measured by ELISA for the FOS(−) (open circles) and FOS(+) diet (closed circles) groups. The results are expressed as the mean ± 1 s.d. ($n = 6$). *Significant difference from the FOS(−) diet group ($P < 0.05$) by two-way ANOVA with Tukey–Kramer's *post hoc* test.

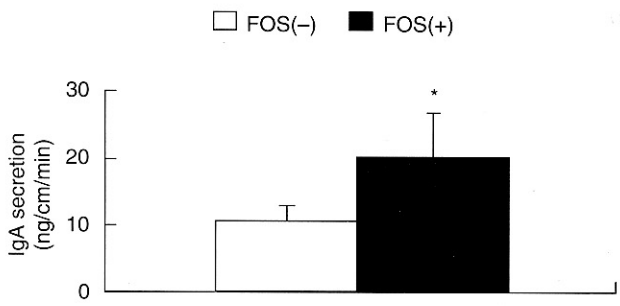

Fig. 2. Effect of dietary FOS on ileal IgA secretion. The results are expressed as the mean + 1 s.d. ($n = 6$). *Significant difference from the FOS(−) diet group ($P < 0.05$) by the Student's *t*-test.

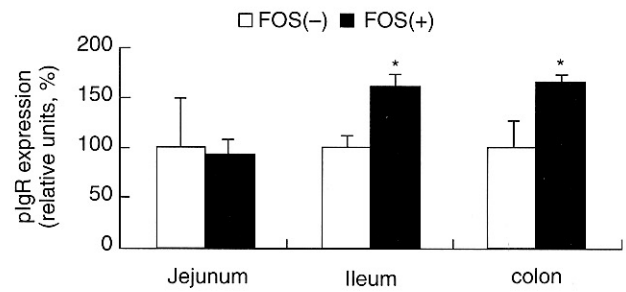

Fig. 3. Effect of dietary FOS on pIgR expression in the jejunum, ileum and colon. The relative quantities of pIgR were estimated by densitometric scanning. The values were expressed relative to the average value in FOS(−) diet group that was normalized to 100. The results are expressed as the mean + 1 s.d. ($n = 3$). *Significant difference from FOS(−) diet group ($P < 0.05$) by the Mann–Whitney *U*-test.

Effect of dietary FOS on the concentration of short-chain fatty acids in the caecum contents

Short-chain fatty acids (mainly acetic, propionic and butyric acids) are formed in the caecum as a result of anaerobic bacterial fermentation of dietary FOS. Mice fed the FOS(+) diet had higher caecum acetate ($P < 0.05$), butyrate ($P < 0.05$) and propionate ($P = 0.09$) concentrations than mice fed the FOS(−) diet (Table 3). These results were consistent with those of previous reports [19].

Effect of dietary FOS on the IgA response and B cell subpopulations in PP

The culture period (7 days) established for PP cells was based on the results of a preliminary time–course study (data not shown). The IgA response of PP cells in the FOS(+) diet group was significantly higher than that in the FOS(−) diet group (89 ± 77 ng/ml *versus* 553 ± 160 ng/ml; $P < 0.05$). This result led us to analyse the percentages of PP cells identified as $B220^+$, IgA^+ and IgM^+ (Table 4). The diet supplemented with FOS did not have any effect on the percentages of $B220^+$ cells in PP. However, the

Table 3. The caecum SCFA concentrations for mice fed FOS(−) or FOS(+) diets[1]

	FOS(−)			FOS(+)		
	Mean	s.d.	*n*	Mean	s.d.	*n*
Acetate (mmol/kg caecum water)	24·6	0·6	5	40·5*	9·6	5
Propionate (mmol/kg caecum water)	5·1	0·5	5	6·4	1·4	5
Butyrate (mmol/kg caecum water)	2·8	0·6	5	7·6*	2·3	5

SCFA: short-chain fatty acid; FOS: fructooligosaccharides; s.d.: standard deviation. [1]The FOS(+) diet includes 5% fructooligosaccharides (Meiji Seika Kaisya, Ltd, Tokyo, Japan) + 95% FOS(−) diet (for details of the FOS(−) diet, see Table 1. *Significant difference from the FOS(−) diet group ($P < 0·05$) by the Student's *t*-test.

Table 4. Peyer's patch B cell subpopulations for mice fed FOS(−) or FOS(+) diets[1]

	FOS(−)			FOS(+)		
	Mean	s.d.	*n*	Mean	s.d.	*n*
$B220^+$ (%)	77·1	2·4	5	77·4	2·9	6
$B220^+IgM^+$ (%)	72·1	2·0	5	71·3	3·4	6
$B220^+IgA^+$ (%)	4·0	1·1	5	6·5*	0·8	6

FOS: fructooligosaccharides; s.d.: standard deviation. [1]The FOS(+) diet includes 5% fructooligosaccharides (Meiji Seika Kaisya, Ltd, Tokyo, Japan) + 95% FOS(−) diet (for details of the FOS(−) diet, see Table 1. *Significant difference from the FOS(−) diet group ($P < 0·05$) by the Student's *t*-test.

percentage of $B220^+IgA^+$ cells was significantly higher in the FOS(+) than the FOS(−) diet group (6·2% vs. 4·3%). The percentage of $B220^+IgM^+$ cells in PP was not significantly different between the two groups.

DISCUSSION

In the present study, we examined whether dietary FOS in infancy can have a beneficial effect on the mucosal immune system. Prebiotics are food products that are designed especially to benefit the host by selectively stimulating the growth and/or activity of one or a limited number of bacterial species already resident in the colon [2,20]. It is assumed that prebiotics usually act in the colon. Most prebiotics resist hydrolysis, reach the colon intact and are fermented extensively in the colon by resident anaerobic bacteria. Thus, it is expected that the immunomodulatory effects of prebiotics would be observed mainly in the colon. Previous studies have shown that dietary FOS reduced the occurrence of colon tumours and trinitrobenzene sulphonic acid hapten-induced chronic colitis [21,22]. Furthermore, Buddington *et al.* [23] reported that diets supplemented with inulin and oligofructose lowered the incidence and growth of tumours in the colon after exposure to carcinogens. In agreement with these studies, our findings indicate that dietary FOS increase the total IgA levels in tissue extracts isolated from the colon and increase pIgR expression in the colon.

Similar to the colon, where solitary lymphoid follicles are present as gut-associated lymphoid tissue (GALT), the small intestine is another site where GALT, such as PP, is located and the mucosal IgA response is induced. In the human small intestine, it has been estimated that there are approximately 10^{10} immunoglobulin-producing cells per metre, most of which produce IgA, accounting for approximately 80% of all immunoglobulin-producing cells in the whole body [24]. Thus, we investigated whether dietary FOS showed a beneficial effect on the mucosal immune response in the small intestine. As demonstrated for the mucosal IgA response in the colon of infant mice, dietary FOS increased the total IgA levels in tissue extracts isolated from the jejunum and ileum ($P < 0·05$) (Table 2). Furthermore, pIgR expression in the ileum was significantly higher in the FOS(+) compared with the FOS(−) diet group. Thus, dietary FOS effect the mucosal immune system in the small intestine of infant mice as well as in the colon. However, the mechanism by which dietary FOS increases the IgA response and pIgR expression in the small intestine remains to be elucidated.

Dietary FOS has been shown to up-regulate the faecal IgA content in adult mice [9]. Our present findings in newborn mice are consistent with this observation. However, unlike humans, pIgR-mediated IgA transport occurs not only in the intestine but also in the liver in rodents [25]. Furthermore, it is possible that secretory IgA may be digested in the intestinal lumen, because some bacterial species have been shown to possess proteases capable of degrading IgA [26]. Therefore, faecal IgA levels may not reflect intestinal IgA secretion accurately, especially in mice. We found that ileal IgA secretion was enhanced significantly in the FOS(+) compared with that in the FOS(−) diet group. This may be due to the fact that both the total IgA level in tissue extracts and pIgR expression in the ileum was significantly higher in the FOS(+) diet group. In contrast, another group has shown that supplementation with FOS alone did not influence ileal IgA secretion in ileum-cannulated dogs [10]. The reason for this discrepancy is unclear. One possible reason, however, lies in the age differences between the experimental animals. In the latter study, the effects of feeding FOS were examined in approximately 3-year-old adult dogs, whose intestinal microflora would be less changeable than those in the newborn mice used in our study. In this regard, it has been reported that oral tolerance, which is considered to be a result of the suppressive mucosal immune response as well as the secretory IgA response, is restored in germ-free mice by reconstitution of the intestinal microflora at the neonatal, but not at a later, stage [27]. Therefore, we speculate that the prebiotic effect on the mucosal immune response can best be observed in newborn animals.

Faecal IgA production has been reported to decrease significantly in mice lacking PP caused by different types of gene targeting [28]. Furthermore, a similar result was obtained in a spontaneous mouse mutant whose PP were completely absent [29]. Therefore, it is likely that the mechanism underlying the prebiotic effect on the mucosal immune response includes the function of PP. We found that the *in vitro* IgA response of PP cells from the FOS(+) diet group was higher than that of the FOS(–) diet group. This is consistent with a previous study showing that dietary FOS up-regulates IgA secretion by PP cells [9]. However, it is possible that the PP B cells switch from IgM to IgA production during the *in vitro* culture period. We therefore performed phenotype analysis of PP lymphocytes by flow cytometry. Dietary FOS increased the percentage of $B220^{+}IgA^{+}$ cells (IgA-committed B cells) ($P < 0{\cdot}05$ compared with the FOS(-) group), suggesting that isotype switching from IgM to IgA in PP B cells might be enhanced *in vivo*. In mice, the peritoneal cavity is a major source of B cells [30]. However, a recent study has suggested that the contribution of B cells in the peritoneal cavity to total intestinal IgA may be limited [31]. Thus, our findings that dietary FOS increased the size of the IgA-committed B cell population in PP suggests that this cell population may be responsible, at least in part, for the observed increase in total IgA level in tissue extracts in the FOS(+) diet group.

It is known that intestinal pIgR plays a critical role in transepithelial transport of intestinal IgA onto mucosal surface. For example, Johansen *et al.* [32] reported a complete lack of active external IgA translocation in pIgR knockout mice. It is known that the expression of intestinal pIgR is strictly regulated during ontogeny in humans and rodents [33,34]. These findings [33,34] demonstrate that the production of pIgR protein in intestinal epithelial cells gradually increases after birth. Furthermore, protein–energy malnutrition depresses the production of pIgR protein in intestinal epithelial cells in the weanling mouse intestine [35,36]. Also, the concentration of pIgR is markedly depressed in the small intestine of iron-deprived newborn rats [37]. Therefore, nutritional factors are likely to affect the production of pIgR protein in intestinal epithelial cells in newborn animals. We found that the butyric acid concentration in the caecal contents was enhanced significantly in the FOS(+) compared with that in the FOS(–) diet group. Because butyric acid has been reported to up-regulate intestinal epithelial production of pIgR protein directly *in vitro*, it is possible that butyric acid production regulates intestinal pIgR expression via the fermentation of FOS *in vivo* [38].

Increasing evidence suggests a relationship between the intestinal microflora and allergy. It has been shown that the proportions of anaerobic bacteria in the intestinal flora are higher in non-allergic than allergic children [39]. In particular, non-allergic children harbour higher counts of bifidobacterium than allergic children [40,41]. Thus, there is a trend to supplement infant formula with substances with bifidogenic effects [42]. This seems to be reasonable, because human milk contains bioactive components that stimulate the growth of bifidobacteria in the intestine, such as oligosaccharides [43]. However, there are few studies on the effects of prebiotics on the mucosal immune system in infancy. Therefore, it is noteworthy that dietary FOS was shown to increase the IgA response and pIgR expression in the intestines of infant mice in this study.

In conclusion, we have demonstrated that dietary FOS increases the total IgA levels in tissue extracts from the jejunum, ileum, and colon in infant mice. Moreover, dietary FOS up-regulated ileal and colonic pIgR expression. Consistent with these results, the ileal IgA secretion rate in the FOS(+) diet group was increased. The percentage of $B220^{+}IgA^{+}$ cells in PP was significantly higher in the FOS(+) compared with the FOS(–) diet group, suggesting that isotype switching from IgM to IgA in PP B cells might be enhanced *in vivo*. Taken together, our findings suggest that dietary FOS increases the intestinal IgA response and pIgR expression in both the small intestine and colon in infant mice.

ACKNOWLEDGEMENTS

We thank Meiji Seika Kaisha, Ltd for providing us with fructooligosaccharides (Meioligo-P®). We also thank Drs M. Totsuka, S. Hoshi and M. Yajima for their helpful suggestions.

REFERENCES

1 Mitsuoka T, Hidaka H, Eida T. Effect of fructo-oligosaccharides on intestinal microflora. Nahrung 1987; **31**:427–36.
2 Cummings JH, Macfarlane GT, Englyst HN. Prebiotic digestion and fermentation. Am J Clin Nutr 2001; **73**:S415–20.
3 Yamamoto Y, Yonekubo A. A survey of physical growth, nutritional intake, fecal properties and morbidity of infants as related to feeding methods (VI). Japn J Child Health 1993; **52**:465–71.
4 Juffrie M. Fructooligosaccharide and diarrhea. Biosci Microflora 2002; **21**:31–4.
5 Hidaka H, Eida T, Takizawa T, Tokunaga T, Tashiro Y. Effects of fructooligosaccharides on intestinal flora and human health. Bifidobacteria Microflora 1986; **5**:35–50.
6 Bouhnik Y, Flourie B, Riottot M *et al.* Effects of fructo-oligosaccharides ingestion on fecal bifidobacteria and selected metabolic indexes of colon carcinogenesis in healthy humans. Nutr Cancer 1996; **26**:21–9.
7 Bouhnik Y, Vahedi K, Achour L *et al.* Short-chain fructo-oligosaccharide administration dose-dependently increases fecal bifidobacteria in healthy humans. J Nutr 1999; **129**:113–6.
8 Pierre F, Perrin P, Champ M, Bornet F, Meflah K, Menanteau J. Short-chain fructo-oligosaccharides reduce the occurrence of colon tumors and develop gut-associated lymphoid tissue in Min mice. Cancer Res 1997; **57**:225–8.
9 Hosono A, Ozawa A, Kato R *et al.* Dietary fructooligosaccharides induce immunoregulation of intestinal IgA secretion by murine Peyer's patch cells. Biosci Biotechnol Biochem 2003; **67**:758–64.
10 Swanson KS, Grieshop CM, Flickinger EA *et al.* Supplemental fructooligosaccharides and mannanoligosaccharides influence immune function, ileal and total tract nutrient digestibilities, microbial populations and concentrations of protein catabolites in the large bowel of dogs. J Nutr 2002; **132**:980–9.
11 Takahashi T, Nakagawa E, Nara T, Yajima T, Kuwata T. Effects of orally ingested *Bifidobacterium longum* on the mucosal IgA response of mice to dietary antigens. Biosci Biotechnol Biochem 1998; **62**:10–5.
12 Ahnen DJ, Singleton JR, Hoops TC, Kloppel TM. Posttranslational processing of secretory component in the rat jejunum by a brush border metalloprotease. J Clin Invest 1986; **77**:1841–8.
13 Laemmli UK. Cleavage of structural proteins during the assembly of the head of bacteriophage T4. Nature 1970; **227**:680–5.
14 deVos T, Dick TA. A rapid method to determine the isotype and specificity of coproantibodies in mice infected with *Trichinella* or fed cholera toxin. J Immunol Meth 1991; **141**:285–8.
15 Takahashi T, Oka T, Iwana H, Kuwata T, Yamamoto Y. Immune response of mice to orally administered lactic acid bacteria. Biosci Biotechnol Biochem 1993; **57**:1557–60.
16 Symersky J, Novak J, McPherson DT, DeLucas L, Mestecky J. Expression of the recombinant human immunoglobulin J chain in *Escherichia coli*. Mol Immunol 2000; **37**:133–40.

17 Hoshi S, Sakata T, Mikuni K, Hashimoto H, Kimura S. Galactosylsucrose and xylosylfructoside alter digestive tract size and concentrations of cecal organic acids in rats fed diets containing cholesterol and cholic acid. J Nutr 1994; **124**:52–60.
18 Mestecky J, Lue C, Russell MW. Selective transport of IgA. Cellular and molecular aspects. Gastroenterol Clin North Am 1991; **20**:441–71.
19 Campbell JM, Fahey GC Jr, Wolf BW. Selected indigestible oligosaccharides affect large bowel mass, cecal and fecal short-chain fatty acids, pH and microflora in rats. J Nutr 1997; **127**:130–6.
20 Berggren AM, Bjorck IM, Nyman EMGL. Short-chain fatty acid content and pH in caecum of rats given various sources of carbohydrates. J Sci Food Agric 1993; **63**:397–406.
21 Pierre F, Perrin P, Bassonga E, Bornet F, Meflah K, Menanteau J. T cell status influences colon tumor occurrence in min mice fed short chain fructo-oligosaccharides as a diet supplement. Carcinogenesis 1999; **20**:1953–6.
22 Cherbut C, Michel C, Lecannu G. The prebiotic characteristics of fructooligosaccharides are necessary for reduction of TNBS-induced colitis in rats. J Nutr 2003; **133**:21–7.
23 Buddington KK, Donahoo JB, Buddington RK. Dietary oligofructose and inulin protect mice from enteric and systemic pathogens and tumor inducers. J Nutr 2002; **132**:472–7.
24 Brandtzaeg P, Halstensen TS, Kett K *et al.* Immunobiology and immunopathology of human gut mucosa: humoral immunity and intraepithelial lymphocytes. Gastroenterology 1989; **97**:1562–84.
25 Brandtzaeg P. Role of J chain and secretory component in receptor-mediated glandular and hepatic transport of immunoglobulins in man. Scand J Immunol 1985; **22**:111–46.
26 Kilian M, Reinholdt J, Lomholt H, Poulsen K, Frandsen EV. Biological significance of IgA1 proteases in bacterial colonization and pathogenesis: critical evaluation of experimental evidence. APMIS 1996; **104**:321–38.
27 Sudo N, Sawamura S, Tanaka K, Aiba Y, Kubo C, Koga Y. The requirement of intestinal bacterial flora for the development of an IgE production system fully susceptible to oral tolerance induction. J Immunol 1997; **159**:1739–45.
28 Spahn TW, Fontana A, Faria AM *et al.* Induction of oral tolerance to cellular immune responses in the absence of Peyer's patches. Eur J Immunol 2001; **31**:1278–87.
29 HogenEsch H, Janke S, Boggess D, Sundberg JP. Absence of Peyer's patches and abnormal lymphoid architecture in chronic proliferative dermatitis (cpdm/cpdm) mice. J Immunol 1999; **162**:3890–6.
30 Kroese FG, Butcher EC, Stall AM, Herzenberg LA. A major peritoneal reservoir of precursors for intestinal IgA plasma cells. Immunol Invest 1989; **18**:47–58.
31 Fagarasan S, Kinoshita K, Muramatsu M, Ikuta K, Honjo T. *In situ* class switching and differentiation to IgA-producing cells in the gut lamina propria. Nature 2001; **413**:639–43.
32 Johansen FE, Pekna M, Norderhaug IN *et al.* Absence of epithelial immunoglobulin A transport, with increased mucosal leakiness, in polymeric immunoglobulin receptor/secretory component-deficient mice. J Exp Med 1999; **190**:915–22.
33 Rognum TO, Thrane S, Stoltenberg L, Vege A, Brandtzaeg P. Development of intestinal mucosal immunity in fetal life and the first postnatal months. Pediatr Res 1992; **32**:145–9.
34 Buts JP, Delacroix DL. Ontogenic changes in secretory component expression by villous and crypt cells of rat small intestine. Immunology 1985; **54**:181–7.
35 Ha CL, Woodward B. Depression in the quantity of intestinal secretory IgA and in the expression of the polymeric immunoglobulin receptor in caloric deficiency of the weanling mouse. Lab Invest 1998; **78**:1255–66.
36 Ha CL, Woodward B. Reduction in the quantity of the polymeric immunoglobulin receptor is sufficient to account for the low concentration of intestinal secretory immunoglobulin A in a weanling mouse model of wasting protein-energy malnutrition. J Nutr 1997; **127**:427–35.
37 Buts JP, Delacroix DL, Dekeyser N *et al.* Role of dietary iron in maturation of rat small intestine at weaning. Am J Physiol 1984; **246**:G725–31.
38 Kvale D, Brandtzaeg P. Constitutive and cytokine induced expression of HLA molecules, secretory component, and intercellular adhesion molecule-1 is modulated by butyrate in the colonic epithelial cell line HT-29. Gut 1995; **36**:737–42.
39 Bjorksten B, Naaber P, Sepp E, Mikelsaar M. The intestinal microflora in allergic Estonian and Swedish 2-year-old children. Clin Exp Allergy 1999; **29**:342–6.
40 Kalliomaki M, Kirjavainen P, Eerola E, Kero P, Salminen S, Isolauri E. Distinct patterns of neonatal gut microflora in infants in whom atopy was and was not developing. J Allergy Clin Immunol 2001; **107**:129–34.
41 Watanabe S, Narisawa Y, Arase S *et al.* Differences in fecal microflora between patients with atopic dermatitis and healthy control subjects. J Allergy Clin Immunol 2003; **111**:587–91.
42 Vandenplas Y. Oligosaccharides in infant formula. Br J Nutr 2002; **87**:S293–6.
43 Kunz C, Rudloff S, Baier W, Klein N, Strobel S. Oligosaccharides in human milk: structural, functional, and metabolic aspects. Annu Rev Nutr 2000; **20**:699–722.